

MULTIPLE SIGNAL CLASSIFICATION METHOD IN DIRECTION OF ARRIVAL ESTIMATION

MUSTAFA SERDAR FIDAN

20322381

HACETTEPE UNIVERSITY

ELECTRICAL-ELETRONICS ENGINEERING DEPARTMENT

ELE 401- ELE 402 FINAL PROJECT REPORT

Instructor : Prof. Dr. FEZA ARIKAN

Spring 2007

Abstract

This report is about **M**ultiple **S**ignal **C**lassification (MUSIC) method which is the most popular technique used in **D**irection **O**f **A**rrival (DOA) estimation. DOA estimation is the work of estimating the direction of an unknown incoming signal to a receiver antenna by some array processing techniques. The report contains a brief data about the MUSIC method, software, outputs gathered with respect to several scenarios executed by the software and conclusions about the performance of Multiple Signal Classification method in DOA estimation due to changing conditions.

Contents

1	Introduction	2
2	Multiple Signal Classification	3
2.1	MUSIC Method	3
2.2	Data Model	3
3	MUSIC Software	5
4	Simulation Results	7
4.1	Simulations with Isotropic Antennas and Synthetic Incoming Signals	7
4.2	Simulations with Ionosphere Channel Simulator	9
4.2.1	Two Close signals incoming to sensor array	9
4.2.2	Two Distinct signals incoming to sensor array	9
4.3	Simulations with RMS Error Calculations	16
4.4	Simulations with Real Data	22
4.4.1	Estimations with original data sets	22
4.4.2	Estimations with concatenated data sets	22
4.4.3	Data Set 23:15:49	22
4.4.4	Data Set 23:06:49	26
5	Conclusion	28
A	Number of Source Estimation	29
B	Standard and Mean Error Calculations For MODLOC 1 and MODLOC 2	30
B.1	SE and ME Calculations For MODLOC 1	30
B.2	SE and ME Calculations For MODLOC 2	30

List of Figures

3.1	Flowchart of Multiple Signal Classification Algorithm	6
4.1	Average Error Comparison for 1 incoming signal to 3 different sensor arrays for different Signal to Noise Ratio levels	8
4.2	Average Error Comparison for 2 distinct incoming signals to 3 different sensor arrays for different Signal to Noise Ratio levels	8
4.3	Average Error Comparison for 2 close incoming signals to 3 different sensor arrays for different Signal to Noise Ratio levels	9
4.4	Average Error Comparison for 2 close signals (MODLOC 1) carrying identical binary sequence messages incoming to sensor arrays for different Signal to Noise Ratio levels under Good Ionosphere Condition	10
4.5	Average Error Comparison for 2 close signals (MODLOC 1) carrying identical binary sequence messages incoming to sensor arrays for different Signal to Noise Ratio levels under Moderate Ionosphere Condition	11
4.6	Average Error Comparison for 2 close signals (MODLOC 1) carrying identical binary sequence messages incoming to sensor arrays for different Signal to Noise Ratio levels under Poor Ionosphere Condition	12
4.7	Average Error Comparison for 2 distinct signals (MODLOC 2) incoming to sensor arrays for different Signal to Noise Ratio levels under Good Ionosphere Condition	13
4.8	Average Error Comparison for 2 distinct signals (MODLOC 2) incoming to sensor arrays for different Signal to Noise Ratio levels under Moderate Ionosphere Condition	14
4.9	Average Error Comparison for 2 distinct signals (MODLOC 2) incoming to sensor arrays for different Signal to Noise Ratio levels under Poor Ionosphere Condition	15
4.10	Path 1 $[35^\circ, 125^\circ]$ and Path 2 $[36^\circ, 123^\circ]$. Signals are incoming onto the V type positioned 5 crossed loop antennas.	16
4.11	Path 1 $[32^\circ, 125^\circ]$, Path 2 $[36^\circ, 125^\circ]$. Signals are incoming onto the V type positioned 5 crossed loop antennas.	17
4.12	Path 1 $[36^\circ, 126^\circ]$, Path 2 $[36^\circ, 122^\circ]$. Signals are incoming onto the V type positioned 5 crossed loop antennas.	18
4.13	Path 1 $[35^\circ, 125^\circ]$, Path 2 $[36^\circ, 123^\circ]$. Signals are incoming onto the 2x2 planar array of crossed loop antennas.	19
4.14	Path 1 $[32^\circ, 125^\circ]$, Path 2 $[36^\circ, 125^\circ]$. Signals are incoming onto the 2x2 planar array of crossed loop antennas.	20
4.15	Path 1 $[36^\circ, 126^\circ]$, Path 2 $[36^\circ, 122^\circ]$. Signals are incoming onto the 2x2 planar array of crossed loop antennas.	21
4.16	Figure denotes the positions of transmitter (Uppsala) and receiver (Kiruna) on the earth. Distance between two positions is 897.16 km.	22
4.17	MUSIC method's elevation estimations with data collected between 23:00:49 and 23:24:49 at two different frequencies	23
4.18	MUSIC method's azimuth estimations with data collected between 23:00:49 and 23:24:49 at two different frequencies	23

4.19	MUSIC method's elevation estimations with concatenated data that is the composition of two data sets with 3 minutes between them collected between 23:00:49 and 23:21:49 at two different frequencies	24
4.20	MUSIC method's azimuth estimations with concatenated data that is the composition of two data sets with 3 minutes between them collected between 23:00:49 and 23:21:49 at two different frequencies	24
4.21	MUSIC Spectrum of Data Set 23:15:49.	25
4.22	MUSIC Spectrum of Data Set 23:15:49.	25
4.23	MUSIC Spectrum of Data Set 23:06:49.	26
4.24	MUSIC Spectrum of Data Set 23:06:49.	27

Chapter 1

Introduction

In signal processing literature, **Direction Of Arrival (DOA)**, denotes the direction from which usually a propagating wave arrives at a point, where usually a set of sensors are located. This set of sensors forms what is called a sensor array. In many signal processing applications a set of unknown parameters should be estimated from measurements collected by array of sensors. DOA estimation of narrow band signals is one example of such applications that has received considerable attention by researchers.[1]

High resolution DOA estimation is important in many applications such as radar, sonar and electronic surveillance. Recent applications include array processing for wireless mobile communications at the base station for increasing the capacity and quality of these systems or design of large space structures. Among the methods proposed for solving the DOA problem, the class of techniques known as signal subspace algorithms is the most promising. These methods by exploiting the underlying data model, try to separate the space spanned by the measured data into what are called noise and signal subspaces. Within this class of algorithms, the method has received the most attention and has been widely studied **MULTIPLE SIGNAL CLASSIFICATION (MUSIC)** algorithm is applicable to arrays with arbitrary geometry and the price paid for this generality is that the array response must be measured and stored for all possible combinations of source parameters.

MUSIC is a method of DOA estimation. MUSIC estimates the DOA content of a signal or autocorrelation matrix using an eigenspace method. This method assumes that a signal, $x(n)$, consists of p complex exponentials in the presence of Gaussian white noise. Given an $L \times L$ autocorrelation matrix, \underline{R} , if the eigenvalues are sorted in decreasing order, the p eigenvectors corresponding to the p largest eigenvalues span the signal subspace.

MUSIC algorithm has many variations.[2] Some of them are Spectral MUSIC, Root-MUSIC, Constrained MUSIC and Beam-space MUSIC. Spectral MUSIC is the most known version of MUSIC and is described briefly in this report. For a **Uniformly spaced Linear Array (ULA)**, the MUSIC spectra can be expressed such that the search for DOA can be made by finding the roots of a polynomial. In this case, the method is known as Root-MUSIC. Constrained MUSIC method incorporates the known source to improve estimates of the unknown source direction. The situation arises when some of the source directions are already known. The method removes signal components induced by these known sources from the data matrix and then uses the modified data matrix for DOA estimation. The MUSIC algorithms discussed so far process the snapshots received from sensor elements without any preprocessing, such as forming beams, and thus may be thought of as element space algorithms, which contrasts with the beam-space MUSIC algorithm in which the array data are passed through a beamforming processor before applying MUSIC or any other DOA estimation algorithms. The beamforming processor output may be thought of as a set of beams; thus, the processing using these data is normally referred to as beam-space processing.

In the report, firstly a brief knowledge about MUSIC method is given. Data model used in calculations are clearly defined and software for 1D estimation and 2D estimation is presented. Simulation results are showed. Conclusions, critics and future ideas are made in the end. Aim of the report is observing the performance of MUSIC method in DOA estimation in 1D and 2D with respect to many changing conditions.

Chapter 2

Multiple Signal Classification

2.1 MUSIC Method

Multiple **S**ignal **C**lassification (MUSIC) is the most popular technique used in Direction of arrival estimation. We can summarize DOA estimation as the work of estimating the direction of an unknown incoming signal to a receiver antenna by some processing techniques.

The MUSIC method is a relatively simple and efficient eigenstructure method of DOA estimation.[3] It has many variations and is perhaps the most studied method in its class. In its standard form, also known as spectral MUSIC., the method estimates the noise subspace from available samples. This can be done by either eigenvalue decomposition of the estimated array correlation matrix or singular value decomposition of the data matrix, with its N columns being the N snapshots of the array signal vectors. The latter is preferred for numerical reasons.

Once the noise subspace has been estimated, a search for angle pairs in the range is made by looking for steering vectors that are orthogonal to the noise subspace as possible. This is normally accomplished by searching for peaks in the MUSIC spectrum.

2.2 Data Model

Sensor array matrix \underline{X} is an l by n matrix where l is the number of sensor antennas and n denotes the number of snapshots taken. Matrix can be formulated as given in the equation 2.1

$$\underline{\underline{X}}^T = [x_1 \dots x_l] \quad (2.1)$$

Total signal induced on the l^{th} element of the receiver array can be formulated by the equation 2.2

$$x_l = \sum_{k=1}^K m_k(t) e^{j2\pi f_0 \tau_l(\theta_k, \phi_k)} + n_l(t) \quad (2.2)$$

Time taken (used as time delay) by the signal to reach the l^{th} element of the receiver array from the reference array element by the k^{th} signal coming from (θ_k, ϕ_k) can be calculated by the equation 2.3

$$\tau_l(\theta_k, \phi_k) = \frac{\vec{r}_l \cdot \hat{\nu}(\theta_k, \phi_k)}{c} \quad (2.3)$$

where

\vec{r}_l denotes the position vector of l^{th} antenna.

$\hat{\nu}(\theta_k, \phi_k)$ denotes the unit vector directed to k^{th} incoming signal.

The autocorrelation matrix of the sensor array can be obtained by the equation 2.4

$$\underline{\underline{R}} = E\{\underline{\underline{X}}\underline{\underline{X}}^T\} \quad (2.4)$$

Find the correlation matrix of the receiver antenna array elements by using the formula given in the equation 2.5 [4].

$$\underline{\underline{R}} = \frac{1}{K} \sum_{n=1}^N x_n x_n^H \quad (2.5)$$

Calculate eigenvalues and eigenvectors of the correlation matrix using equation: Compose a noise subspace matrix which is eigenvectors that corresponds to smallest eigenvalues of the correlation matrix.

For both of all theta and phi angles, create Steering Vector by using the formula given in the equation 2.6.

$$\underline{\underline{s}}(\theta, \phi) = [e^{j2\pi f_0 \tau_1(\theta, \phi)} \dots e^{j2\pi f_0 \tau_l(\theta, \phi)}] \quad (2.6)$$

Calculate P_{MU} for all angle values by using 2.7. Peaks of the MUSIC spectrum are the estimated DOA angles.

$$P_{MU}(\theta, \phi) = \frac{1}{|\underline{\underline{s}}^H(\theta, \phi)\underline{\underline{U}}_L|^2} \quad (2.7)$$

where

$\underline{\underline{U}}_L$ denotes an l by $l - m$ dimensional matrix with its $l - m$ columns being the eigenvectors corresponding to the $l - m$ smallest eigenvalues of the array correlation matrix.

$\underline{\underline{s}}^H(\theta, \phi)$ is the hermitian (transpose of complex conjugate) of the steering vector that is used for scanning the range of meaningful angles for the user.

Chapter 3

MUSIC Software

The software is used to simulate DOA estimation by using **M**ultiple **S**ignal **C**lassification (MUSIC) method. Software is developed in MATLAB. Number of sensors/antennas, signal frequency, sampling frequency, number of samples, number of incident signals can be chosen by the user and can be adjusted easily.

Software uses V_{OC} matrix that is an output of the Ionosphere channel simulation. Frequency, DOA and mode data of the incoming signals are supplied by Ionosphere channel simulation and the data is used directly by MUSIC software. MUSIC spectrum is given as output of the software.

Flowchart of the MUSIC spectrum is shown in the below figure. Searching section is known as brute force searching. θ and ϕ values are incremented as much as the step size that is under control of the user, in each loop and spectrum spans the area ($0^\circ \leq \theta \leq 90^\circ$ and $0^\circ \leq \phi \leq 360^\circ$).

Angles are initialized at the beginning of the software and many calculations in order to find a sensible noise subspace matrix follow the initialization. Search routine can be reduced for saving time or step size can be raised for saving time but the second one reduces resolution and obviously effects DOA estimations.

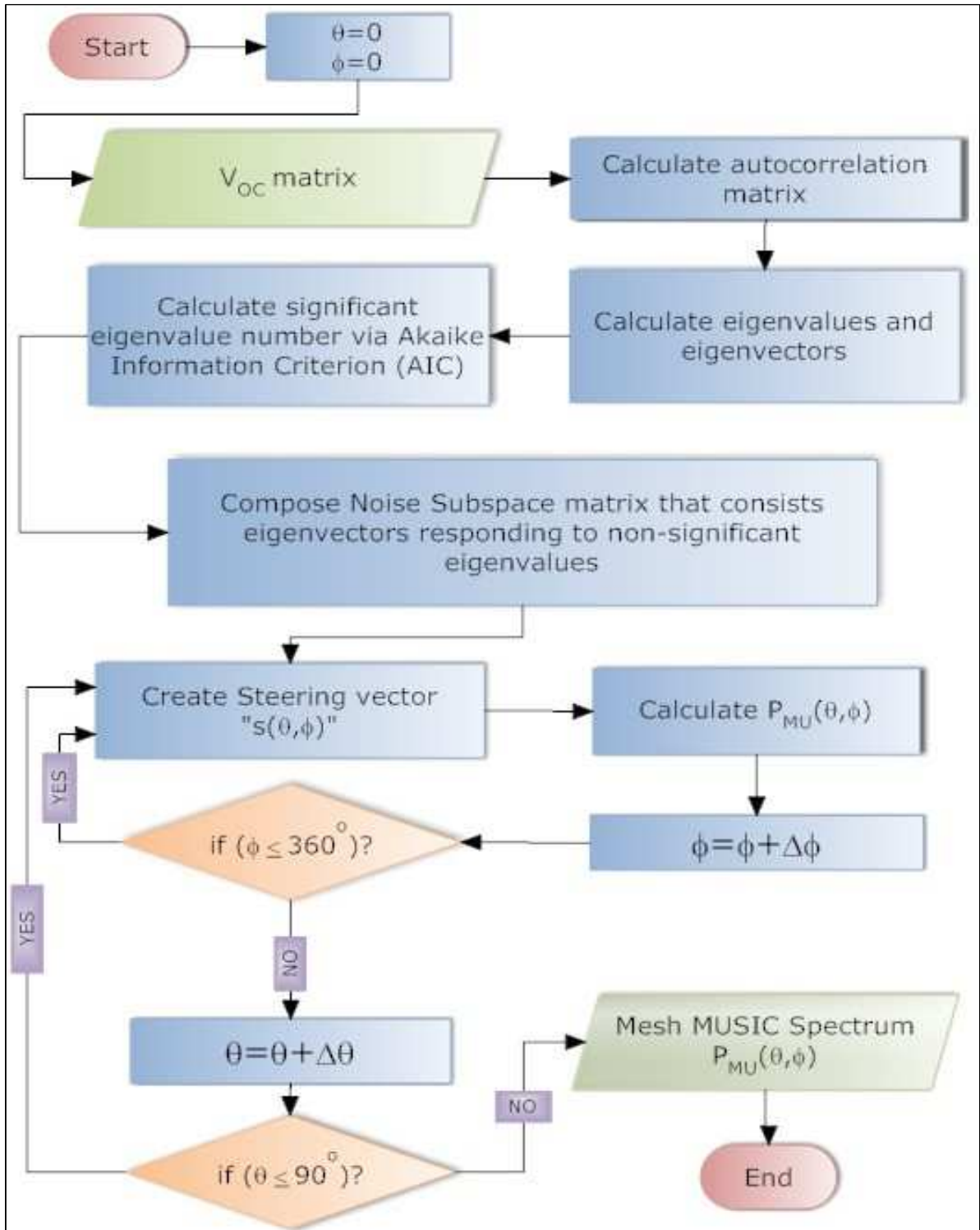


Figure 3.1: Flowchart of Multiple Signal Classification Algorithm

Chapter 4

Simulation Results

Simulations are made in two sections. The first one is "Simulations with Isotropic Antennas". In this section ionosphere conditions are neglected. The second is "Simulations under Ionosphere". Antenna type parameters, array configuration parameters and ionosphere conditions are present in this section.

For all of the simulations Average Errors are calculated and showed in the following figures. Formula for Average Error calculation is :

$$AverageError = \frac{1}{T} \sum_{t=1}^T \sqrt{(\theta_{et1} - \theta_1)^2 + (\phi_{et1} - \phi_1)^2} + \dots + \sqrt{(\theta_{etK} - \theta_K)^2 + (\phi_{etK} - \phi_K)^2} \quad (4.1)$$

where

et: estimated angle value for t^{th} trial

T: number of trials

K: number of incident signals

It is inevitable that when number of incident signals increases, average error will be greater but for the same conditions for all scenarios it gives us chance for comparisons.

4.1 Simulations with Isotropic Antennas and Synthetic Incoming Signals

In the first simulation, one incoming signal at a frequency of 6.175 MHz is synthetically created. Angles of arrival is set to $\theta=55^\circ$ and $\phi=123^\circ$ with respect to sensor array spherical coordinate system. Message signal is pure cosine signal. Snapshots are taken at Nyquist rate. Antenna type is set to isotropic for all of the sensor array configuration. Average error calculations are made with 50 trials for each specification. Error graphic is shown in the figure 4.1.

In this simulation, two distinct incoming signals are sent to sensor array at a frequency of 6.175 MHz. Angles of arrival is set to $\theta_1=55^\circ, \phi_1=123^\circ$ and $\theta_2=45^\circ, \phi_2=130^\circ$ with respect to sensor array spherical coordinate system. Message signals are pure cosine signals and they are not identical. Snapshots are taken at Nyquist rate. Antenna type is set to isotropic for all of the sensor array configuration. Average error calculations are made with 50 trials for each specification. Error graphic is shown in the figure 4.2.

In the last simulation with isotropic antennas, two close incoming signals are sent to sensor array at a frequency of 6.175 MHz. Angles of arrival is set to $\theta_1=51.0^\circ, \phi_1=123.0^\circ$ and $\theta_2=54.2^\circ, \phi_2=123.8^\circ$ with respect to sensor array spherical coordinate system. Message signals are pure cosine signals and they are not identical. Snapshots are taken at Nyquist rate. Antenna type is set to isotropic for all of the sensor array configuration. Average error calculations are made with 50 trials for each specification. Error graphic is shown in the figure 4.3.

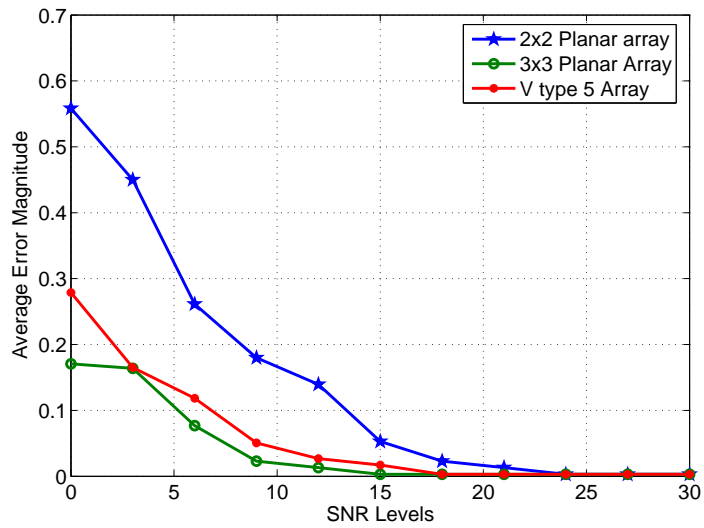


Figure 4.1: Average Error Comparison for 1 incoming signal to 3 different sensor arrays for different Signal to Noise Ratio levels

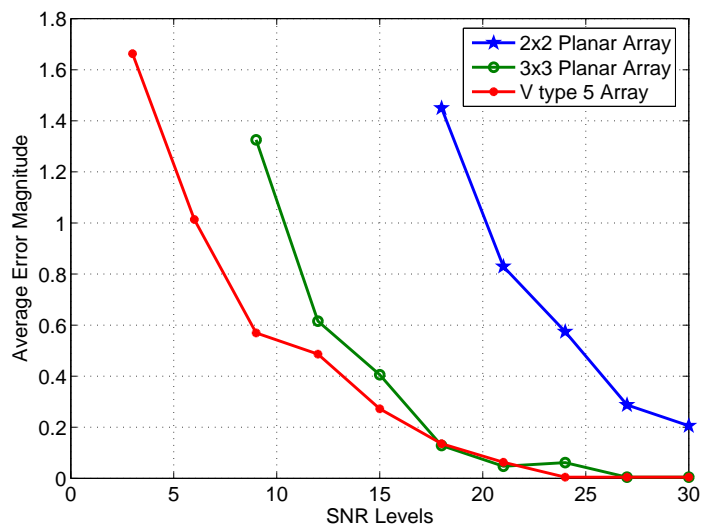


Figure 4.2: Average Error Comparison for 2 distinct incoming signals to 3 different sensor arrays for different Signal to Noise Ratio levels

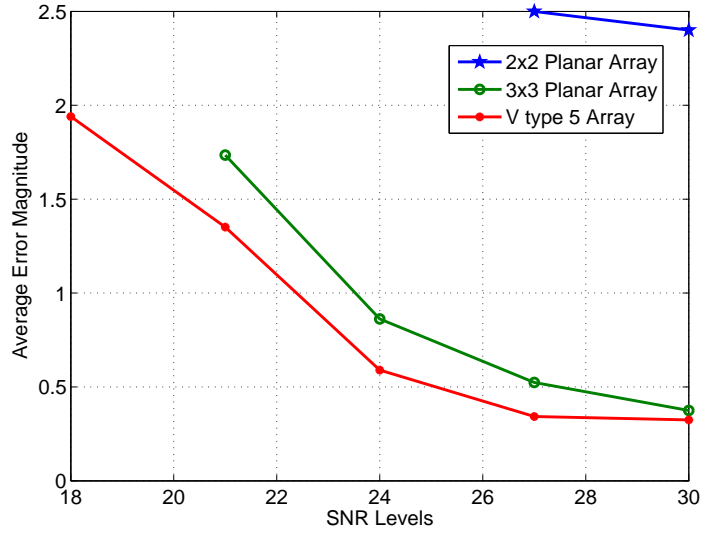


Figure 4.3: Average Error Comparison for 2 close incoming signals to 3 different sensor arrays for different Signal to Noise Ratio levels

4.2 Simulations with Ionosphere Channel Simulator

Input File	Frequency (MHz)	Azimuth (Degree)	Elevation (Degree)	Virtual Height Reflection (km)
MODLOC 1	6.175	123.0, 123.8	51.0, 54.2	209.2, 235.6
MODLOC 2	6.175	105.5, 115.7	51.7, 46.6	214.7, 178.7

Above table shows the specifications of the input files used in the simulations. Azimuth and elevation angles are given with respect to the spherical coordinates that reference antenna is located at origin.

In this section, incoming signals to sensor arrays passed through an Ionosphere channel simulation. Carrier frequency is set to 6.175 MHz. Snapshots are taken at Nyquist rate. 3 different sensor array configurations (2 by 2 Planar array, 3 by 3 Planar array, V type 5 array) and 3 different antenna types (Crossed Loop, Vertical Dipole, Tripole) are used in the simulations. Ionosphere condition is chose as the dominant parameter for simulations and average error calculations are made for 3 ionosphere conditions.

4.2.1 Two Close signals incoming to sensor array

Below figures show the root mean square errors of the simulations that 2 close signals incoming to the sensor arrays (2 by 2 Planar, 3 by 3 Planar, V type 5) under 3 different ionosphere conditions. MODLOC 1 is used as input file that is specified before. Average error graphics are shown in the figure 4.4 (Good Ionosphere), figure 4.5 (Moderate Ionosphere), figure 4.6 (Poor Ionosphere).

4.2.2 Two Distinct signals incoming to sensor array

Below figures show the root mean square errors of the simulations that 2 distinct signal incoming to the sensor arrays (2 by 2 Planar, 3 by 3 Planar, V type 5) under 3 different ionosphere conditions. MODLOC 2 is used as input file that is specified before. Average error graphics are shown in the figure 4.7 (Good Ionosphere), figure 4.8 (Moderate Ionosphere), figure 4.9 (Poor Ionosphere).

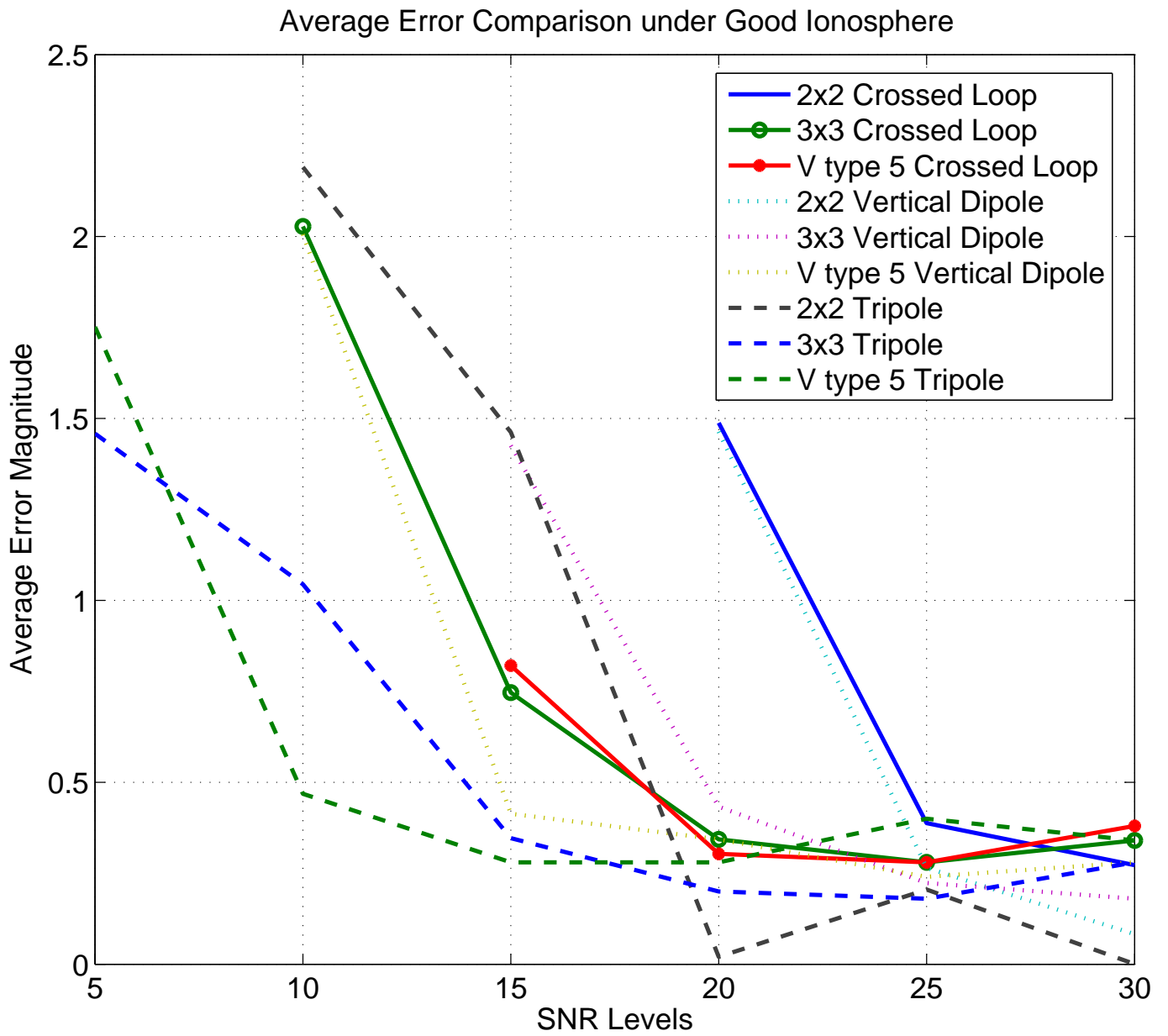


Figure 4.4: Average Error Comparison for 2 close signals (MODLOC 1) carrying identical binary sequence messages incoming to sensor arrays for different Signal to Noise Ratio levels under Good Ionosphere Condition

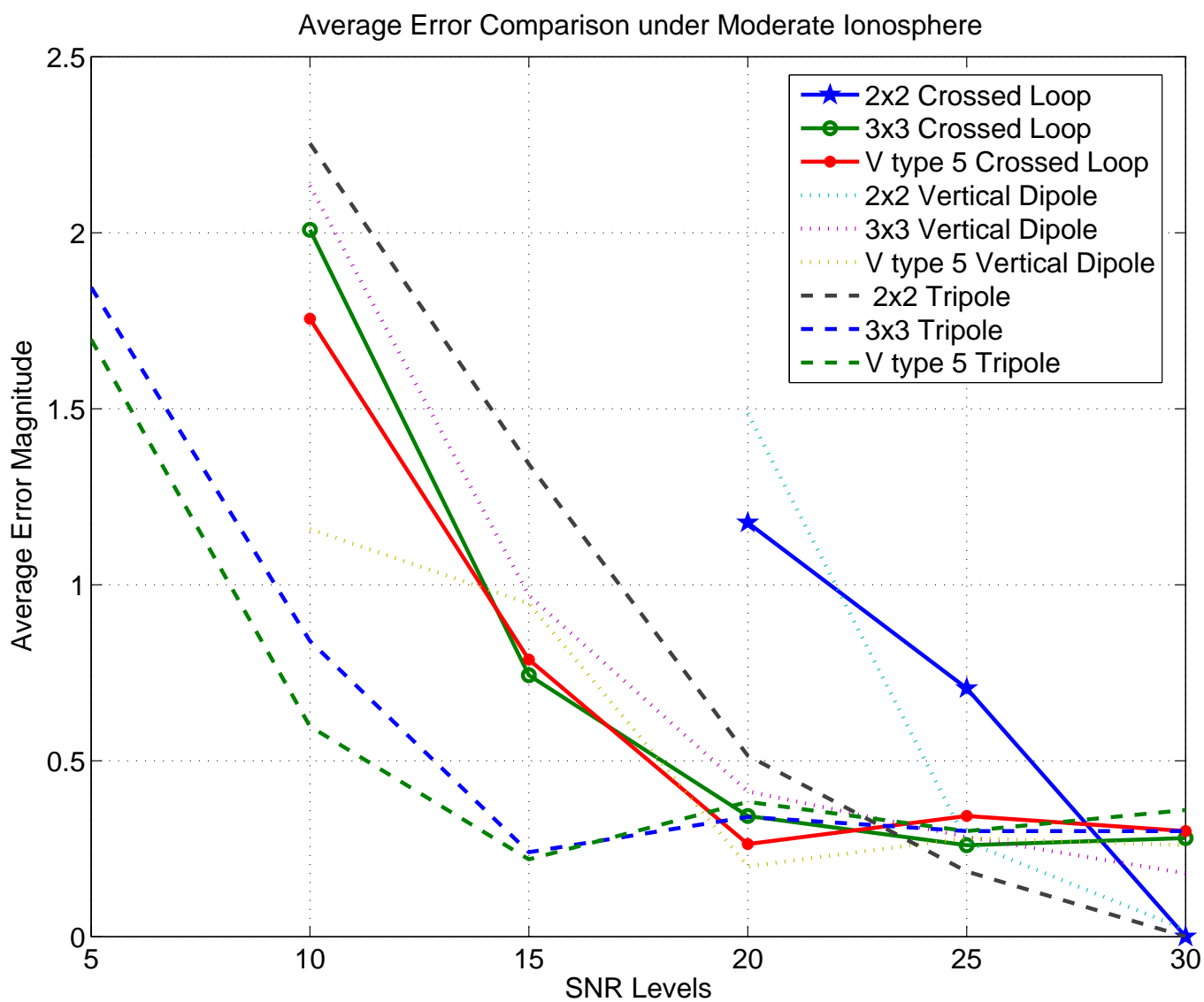


Figure 4.5: Average Error Comparison for 2 close signals (MODLOC 1) carrying identical binary sequence messages incoming to sensor arrays for different Signal to Noise Ratio levels under Moderate Ionosphere Condition

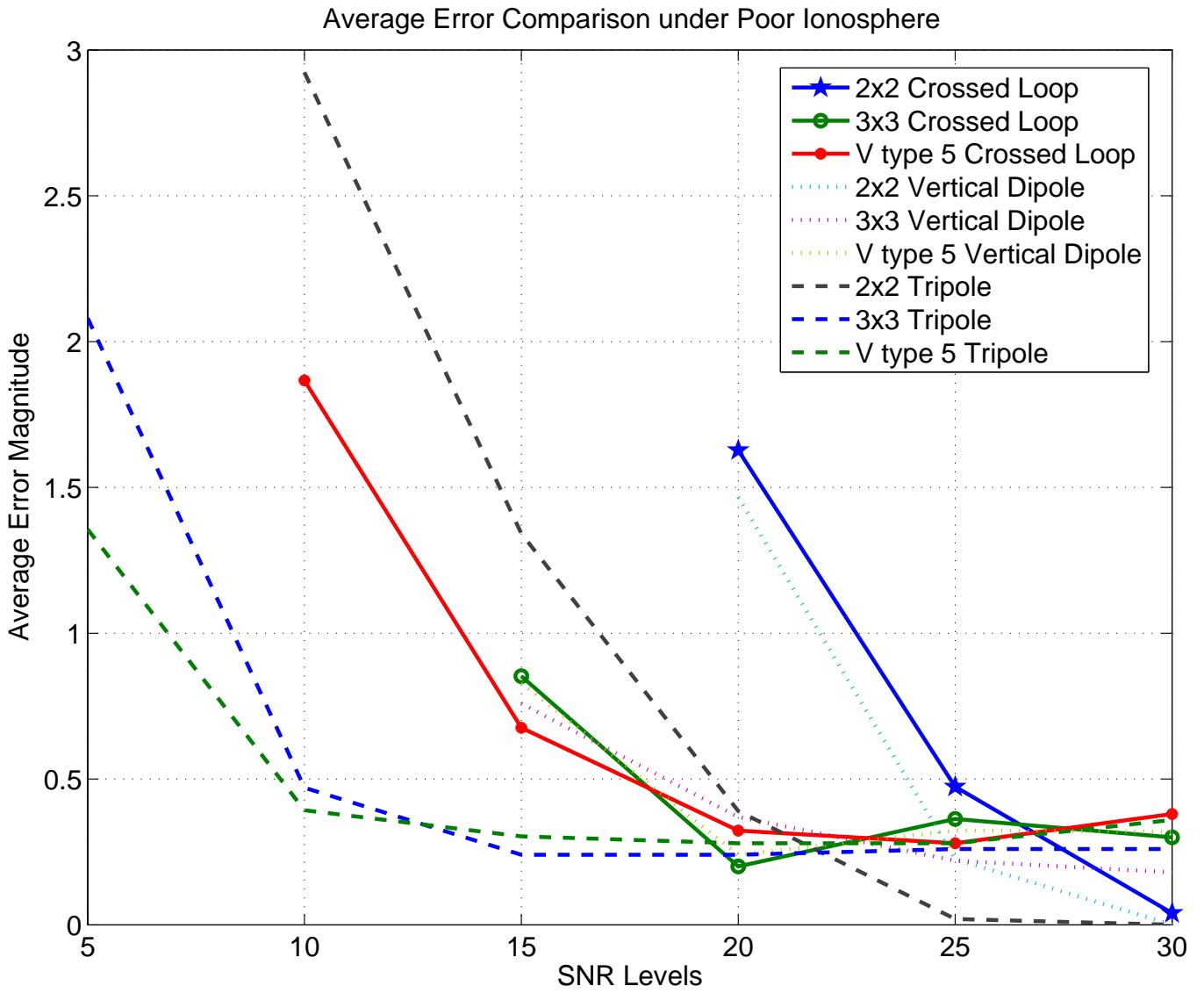


Figure 4.6: Average Error Comparison for 2 close signals (MODLOC 1) carrying identical binary sequence messages incoming to sensor arrays for different Signal to Noise Ratio levels under Poor Ionosphere Condition

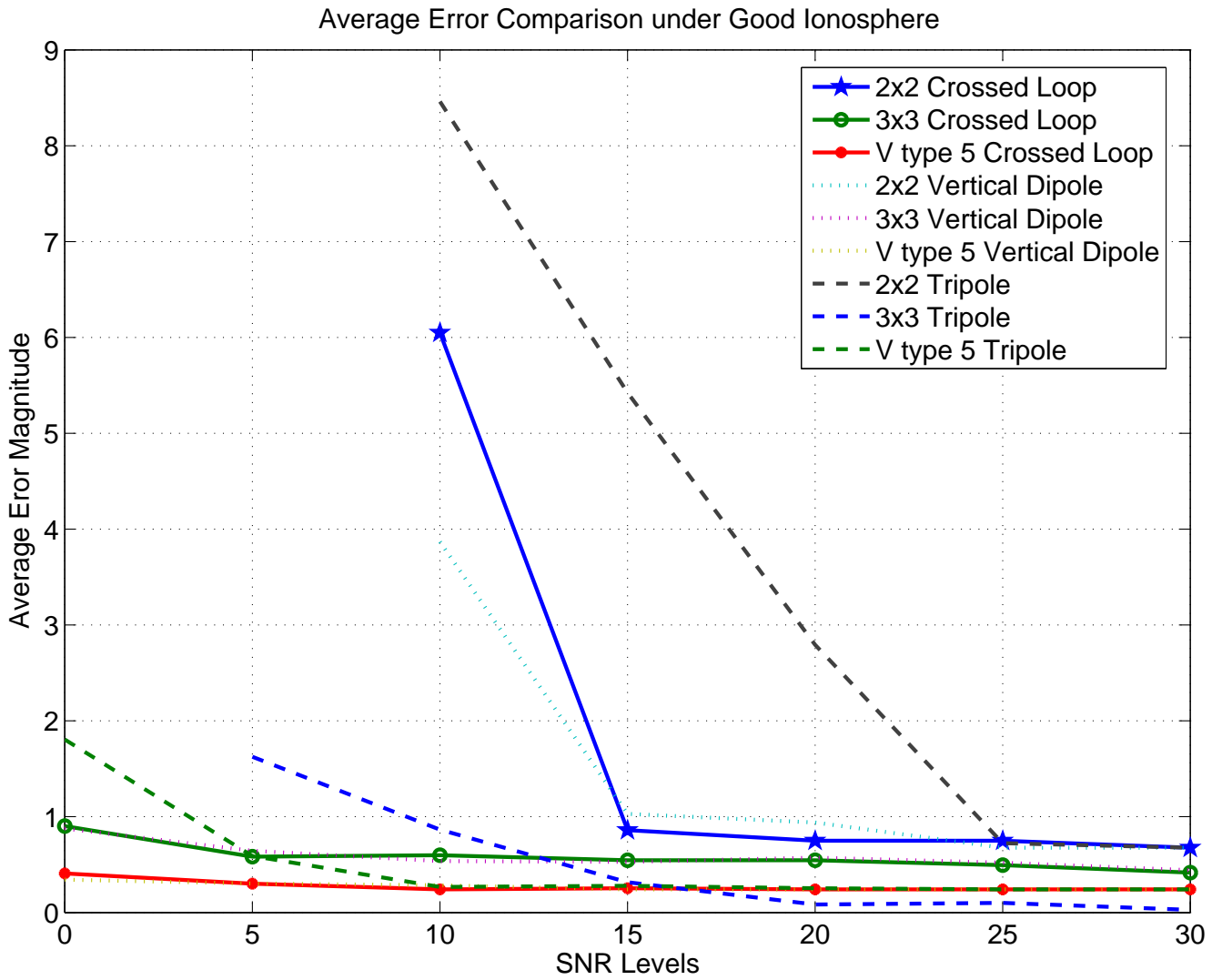


Figure 4.7: Average Error Comparison for 2 distinct signals (MODLOC 2) incoming to sensor arrays for different Signal to Noise Ratio levels under Good Ionosphere Condition

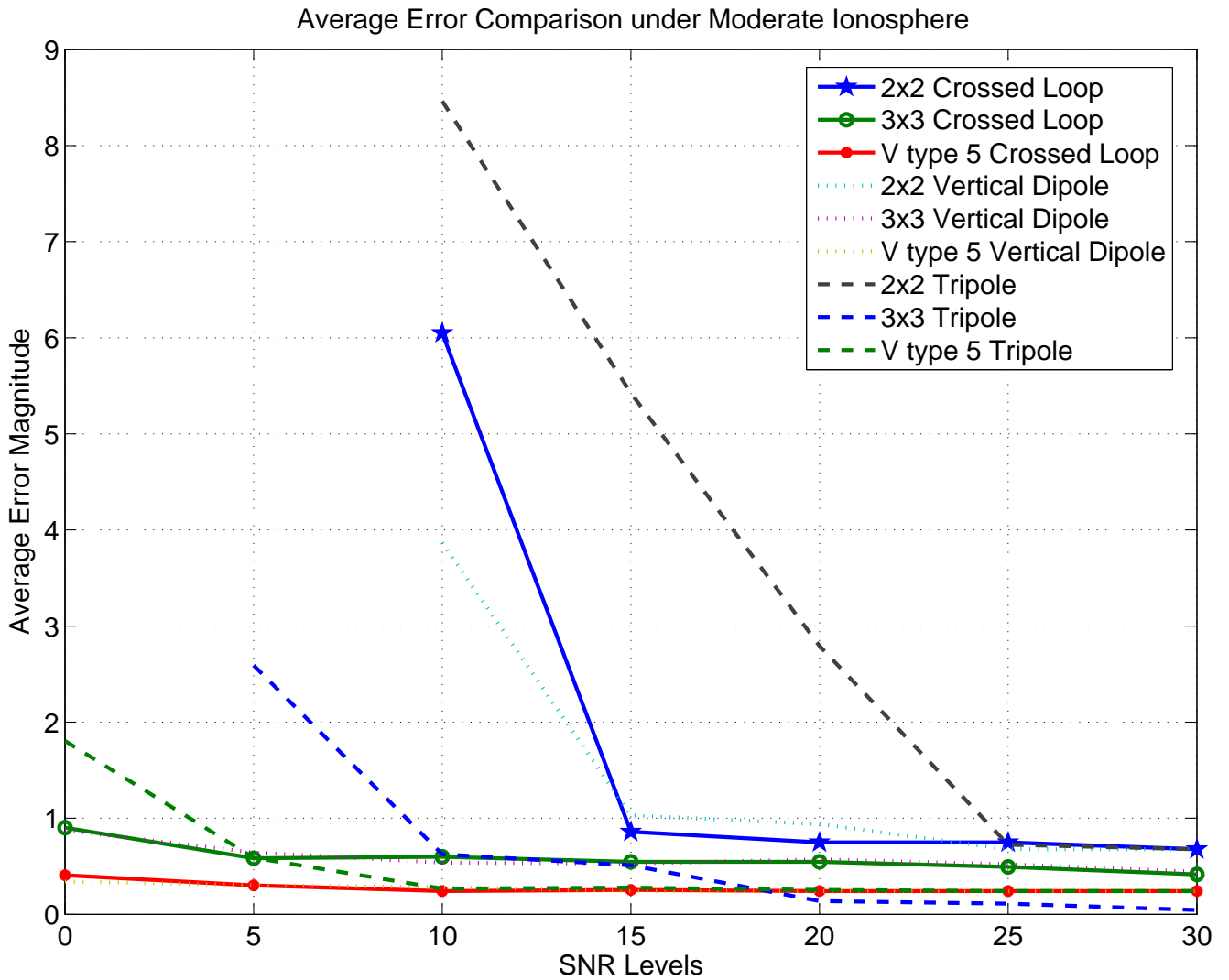


Figure 4.8: Average Error Comparison for 2 distinct signals (MODLOC 2) incoming to sensor arrays for different Signal to Noise Ratio levels under Moderate Ionosphere Condition

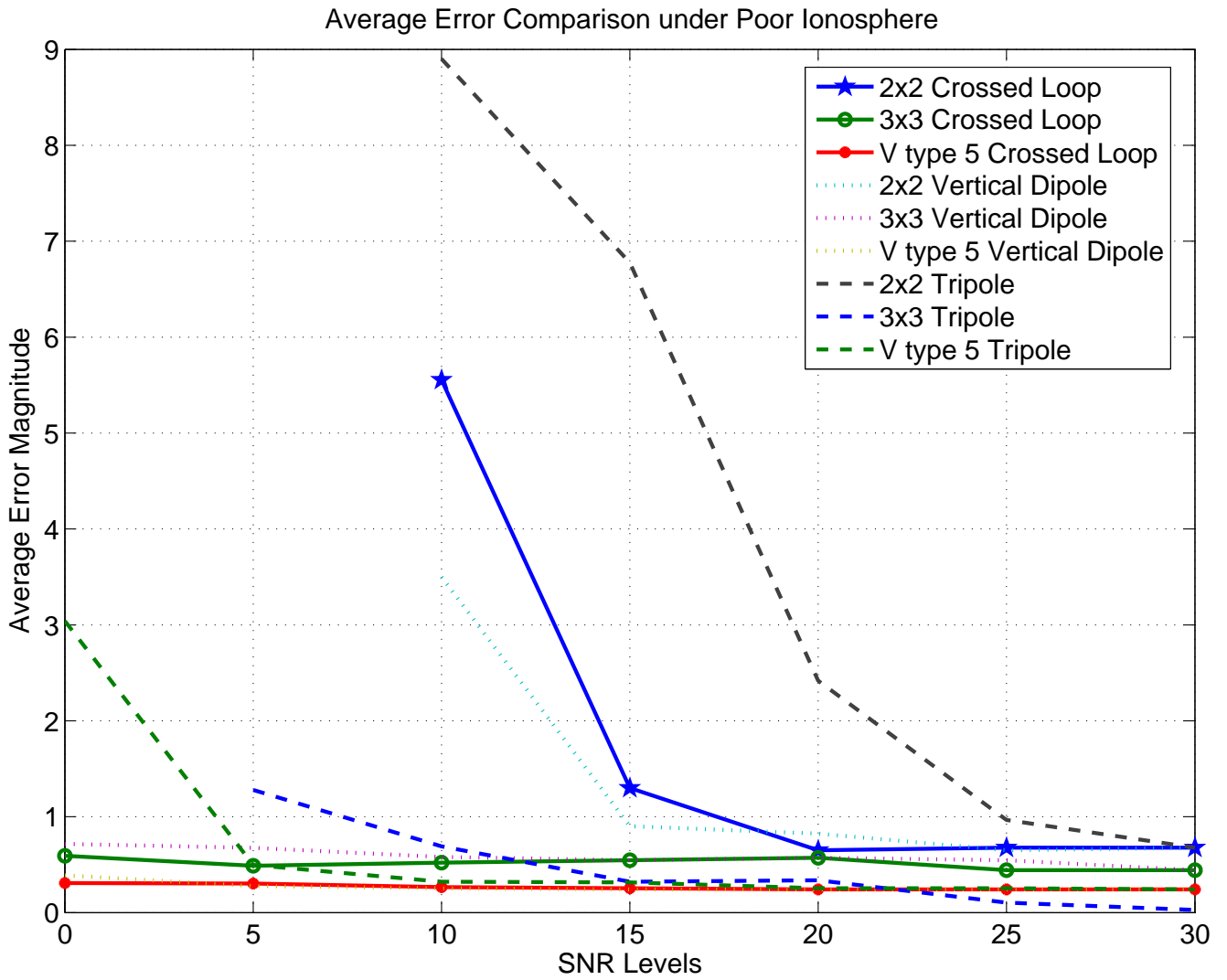


Figure 4.9: Average Error Comparison for 2 distinct signals (MODLOC 2) incoming to sensor arrays for different Signal to Noise Ratio levels under Poor Ionosphere Condition

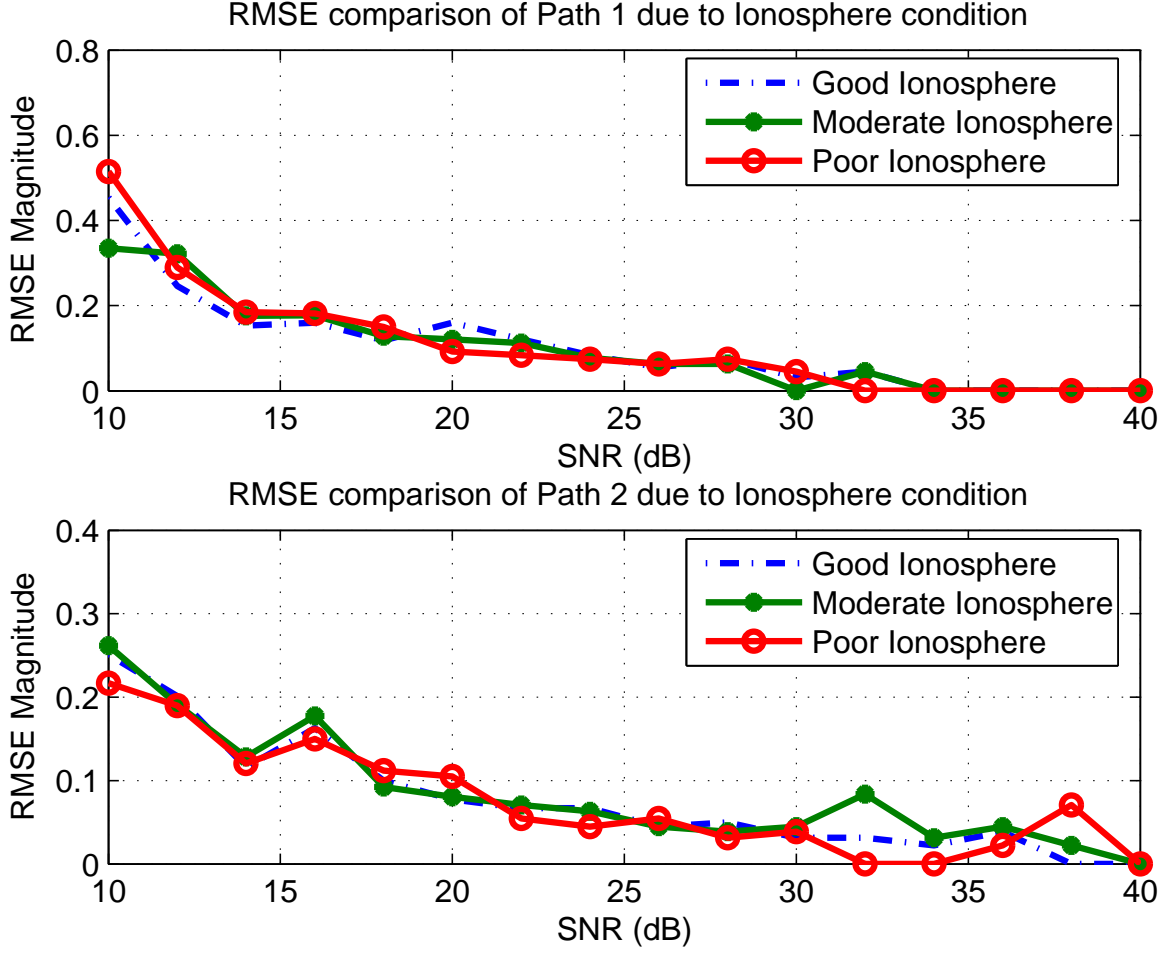


Figure 4.10: Path 1 $[35^\circ, 125^\circ]$ and Path 2 $[36^\circ, 123^\circ]$. Signals are incoming onto the V type positioned 5 crossed loop antennas.

4.3 Simulations with RMS Error Calculations

In this section another error formula is used for comparisons. This formula is defined in the equation 4.2.

$$RMSE = \sqrt{\left[\frac{1}{T} \sum_{t=1}^T ((\widehat{\theta}_{1,t} - \theta_{01})^2 + (\widehat{\phi}_{1,t} - \phi_{01})^2) \right]} \quad (4.2)$$

T : Number of trials

θ_{01}, ϕ_{01} : True values of the elevation and azimuth angles of the path.

$\widehat{\theta}_{1,t}, \widehat{\phi}_{1,t}$: Estimated values of elevation and azimuth angles in the t^{th} trial.

In this section, two different arrays (2x2 Planar array, V type array of 5 antennas) are used for simulations and three different ionosphere conditions (Good, Moderate, Poor) are observed. In all simulations, crossed loop antennas are used. There are two signals used in all simulations with a frequency of $6.175MHz$. Paths are defined under the figures for all simulations. Random binary sequences are used as message signals. Figure 4.10 - figure 4.15 are the results of this section.

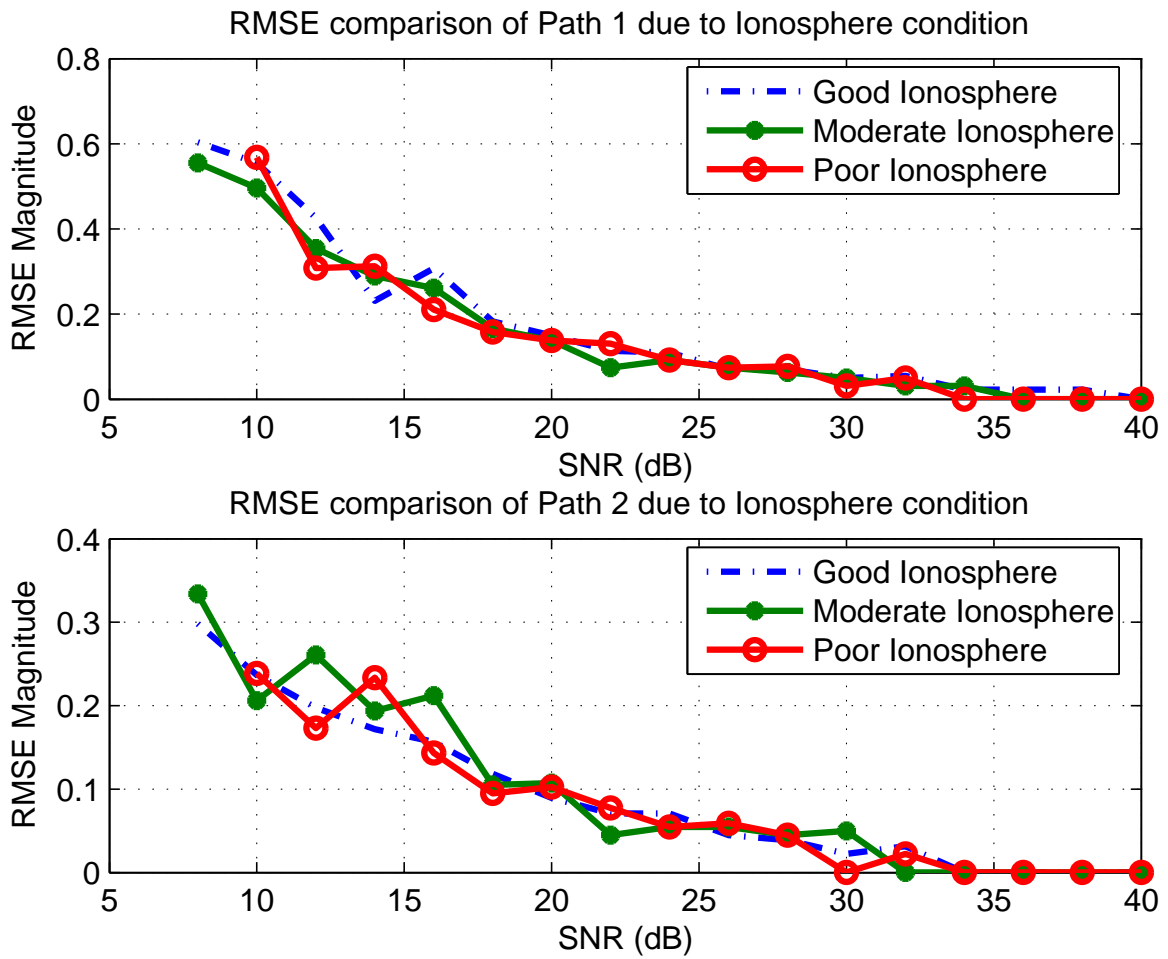


Figure 4.11: Path 1 $[32^\circ, 125^\circ]$, Path 2 $[36^\circ, 125^\circ]$. Signals are incoming onto the V type positioned 5 crossed loop antennas.

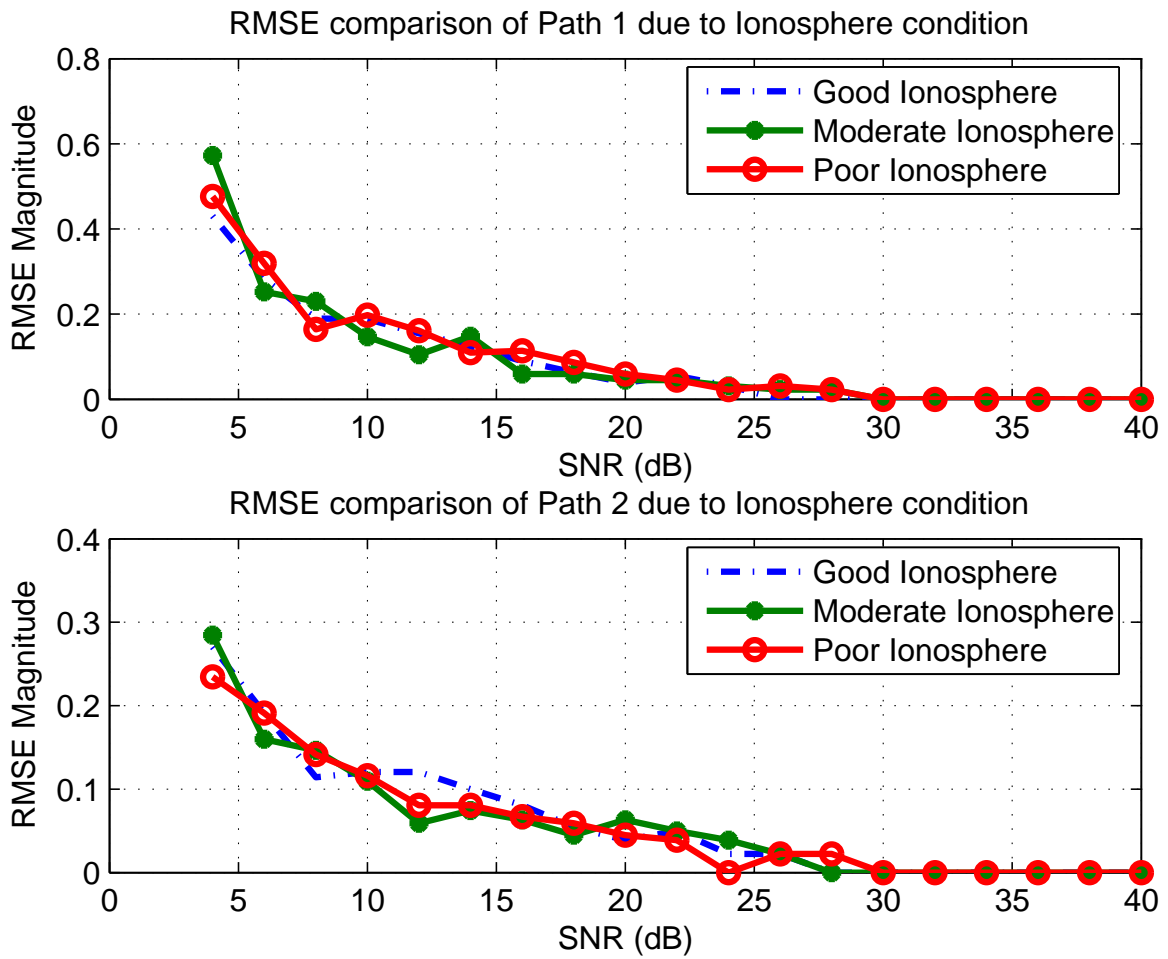


Figure 4.12: Path 1 $[36^\circ, 126^\circ]$, Path 2 $[36^\circ, 122^\circ]$. Signals are incoming onto the V type positioned 5 crossed loop antennas.

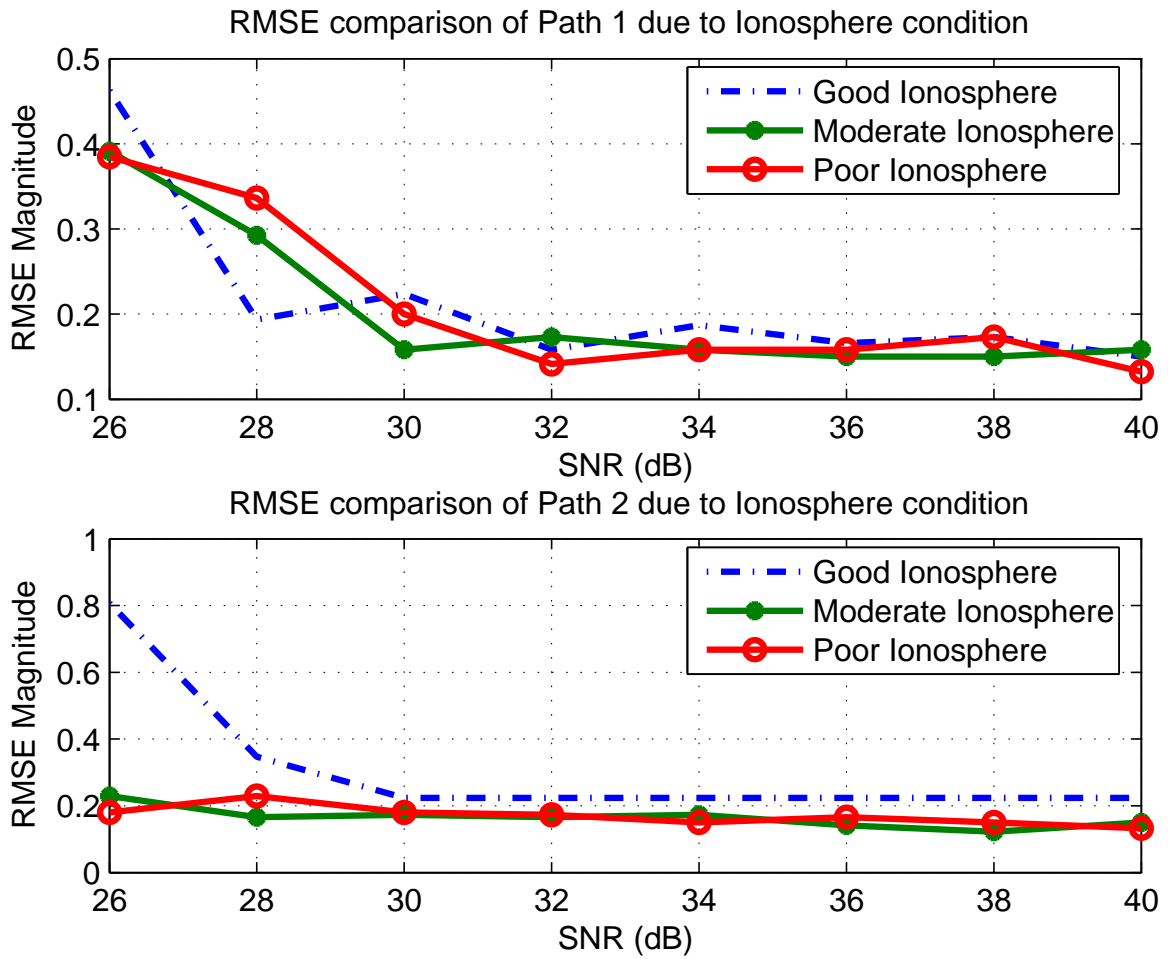


Figure 4.13: Path 1 $[35^\circ, 125^\circ]$, Path 2 $[36^\circ, 123^\circ]$. Signals are incoming onto the 2x2 planar array of crossed loop antennas.

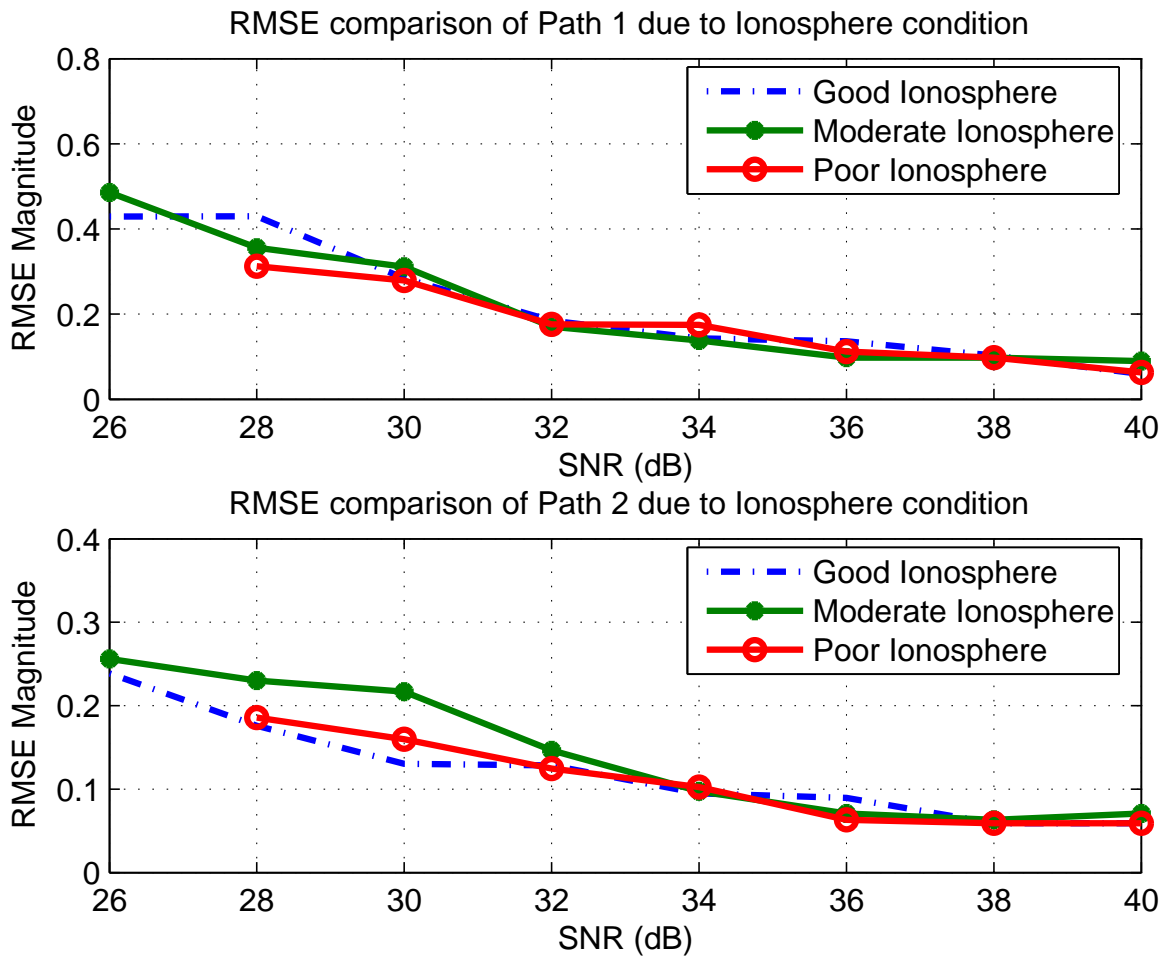


Figure 4.14: Path 1 $[32^\circ, 125^\circ]$, Path 2 $[36^\circ, 125^\circ]$. Signals are incoming onto the 2×2 planar array of crossed loop antennas.

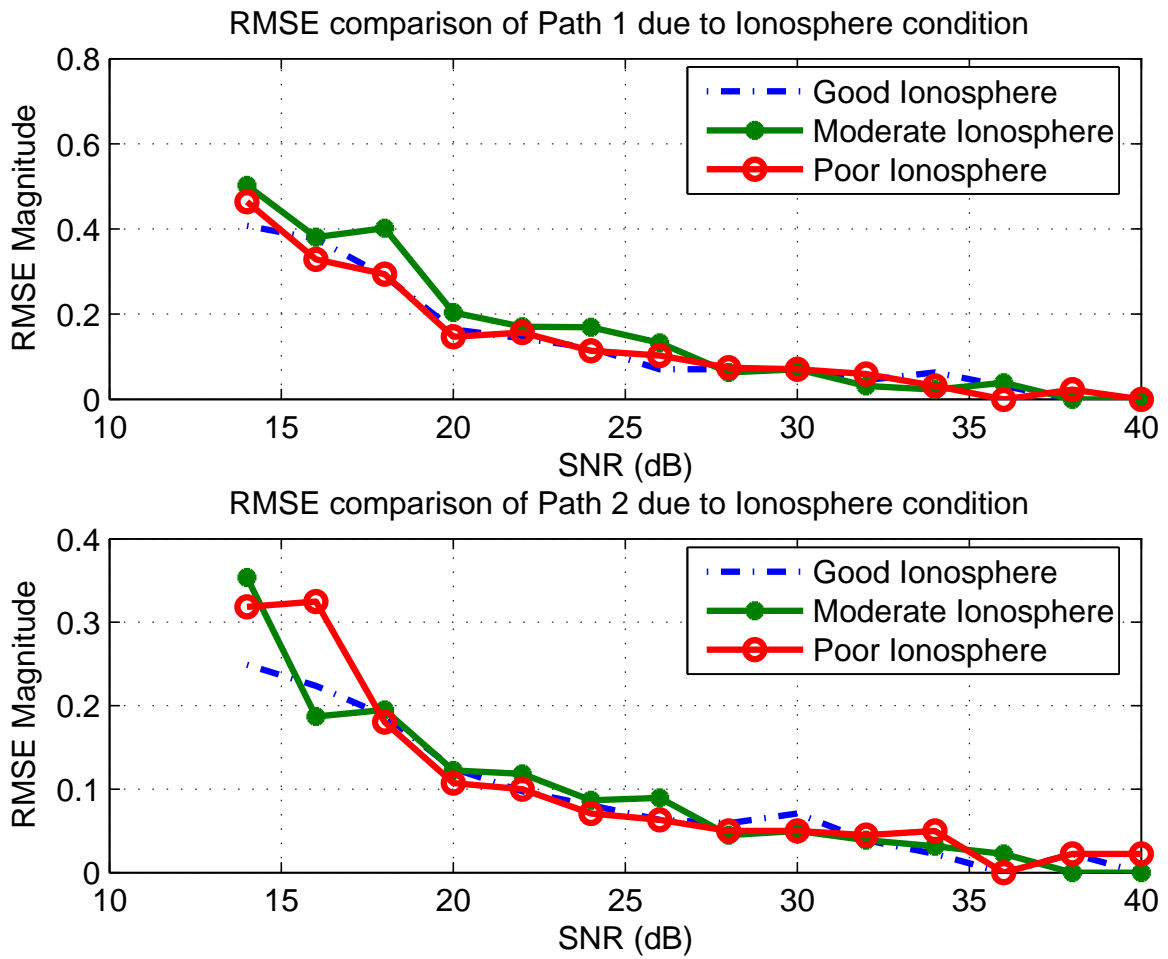


Figure 4.15: Path 1 $[36^\circ, 126^\circ]$, Path 2 $[36^\circ, 122^\circ]$. Signals are incoming onto the 2×2 planar array of crossed loop antennas.



Figure 4.16: Figure denotes the positions of transmitter (Uppsala) and receiver (Kiruna) on the earth. Distance between two positions is 897.16 km.

4.4 Simulations with Real Data

In this section, results of MUSIC algorithm applied on real ionospheric signals recorded by the University of Leister, Electrical and Electronics Department will be presented.

The signals processed in the simulations were radiated by a **D**oppler and **M**ultipath **S**ounding **N**etwork (DAMSON) transmitter which is the result of a collaboration between the UK Defence Evaluation and Research Agency, the Canadian Communications Research Center, the Norwegian Defence Research Establishment and the Swedish Defence Research Establishment. This system characterizes the propagation path using a number of sounding signals which can be freely scheduled.

4.4.1 Estimations with original data sets

Transmitter sends messages that have durations of 2 seconds with 3 minutes intervals at the same frequency. There are 9 data sets for each of these two frequencies. Data sets are collected between 23:00:49 and 23:24:49.

4.4.2 Estimations with concatenated data sets

In this section 2 data sets are concatenated and MUSIC is applied on this new data set.

4.4.3 Data Set 23:15:49

In this section, data set collected at 23:15:49 is used. Open circuit voltage outputs of 5 antenna positioned circularly are used in estimations. Frequency is 6.95MHz . Below figures show the MUSIC method's estimation in 3D and 2D plots. Spectrum clarifies that there is one incoming signal from elevation 33.3° and azimuth 197.4° .

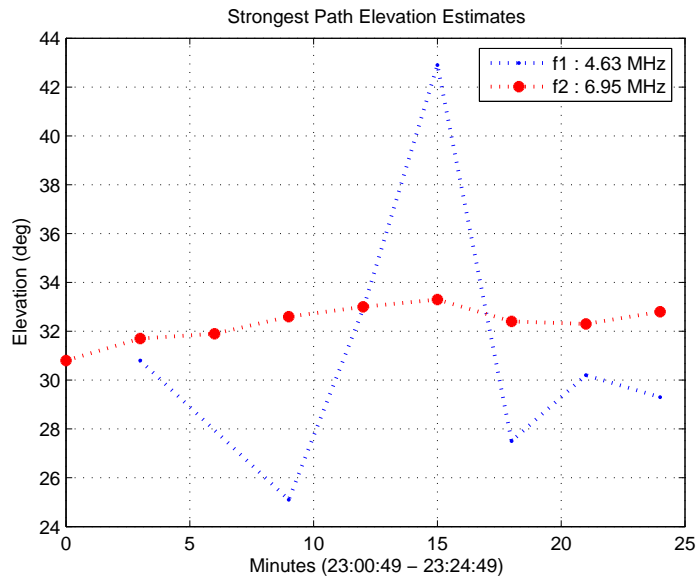


Figure 4.17: MUSIC method's elevation estimations with data collected between 23:00:49 and 23:24:49 at two different frequencies .

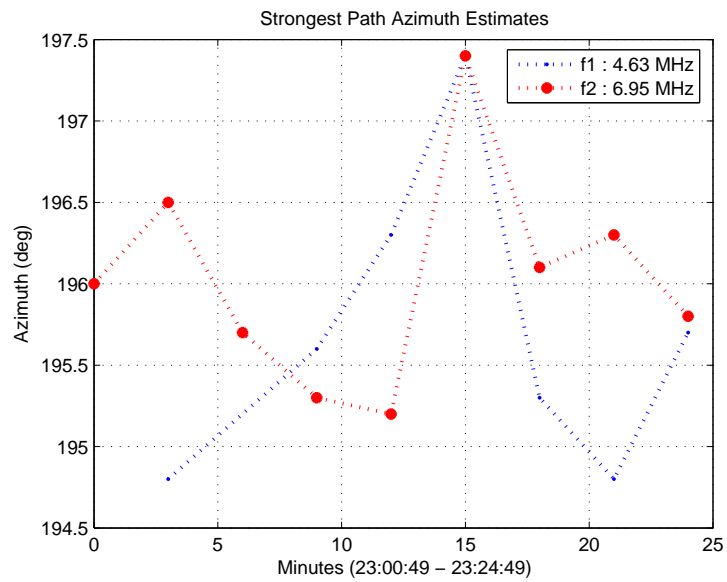


Figure 4.18: MUSIC method's azimuth estimations with data collected between 23:00:49 and 23:24:49 at two different frequencies .

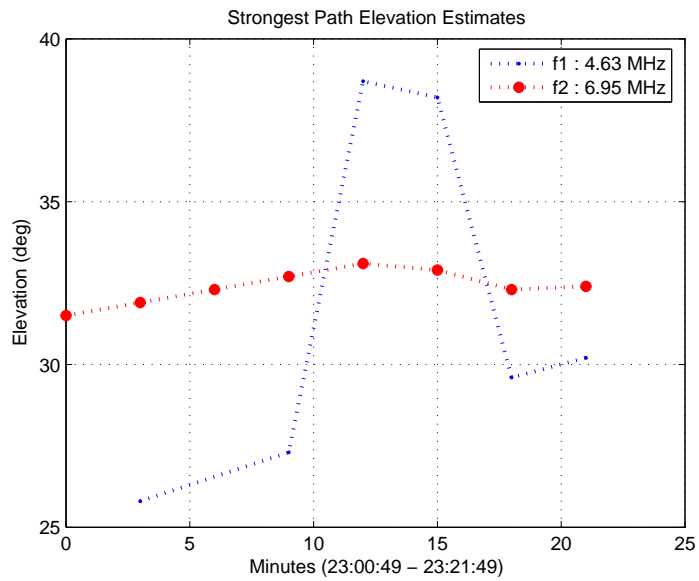


Figure 4.19: MUSIC method's elevation estimations with concatenated data that is the composition of two data sets with 3 minutes between them collected between 23:00:49 and 23:21:49 at two different frequencies

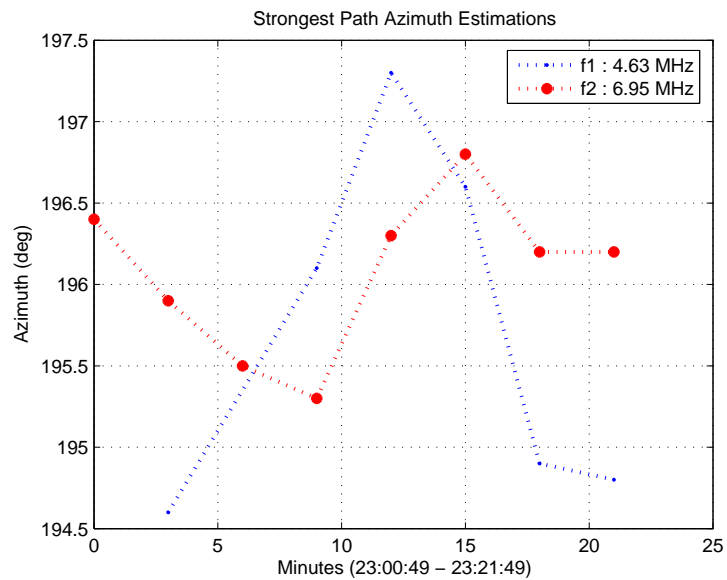


Figure 4.20: MUSIC method's azimuth estimations with concatenated data that is the composition of two data sets with 3 minutes between them collected between 23:00:49 and 23:21:49 at two different frequencies

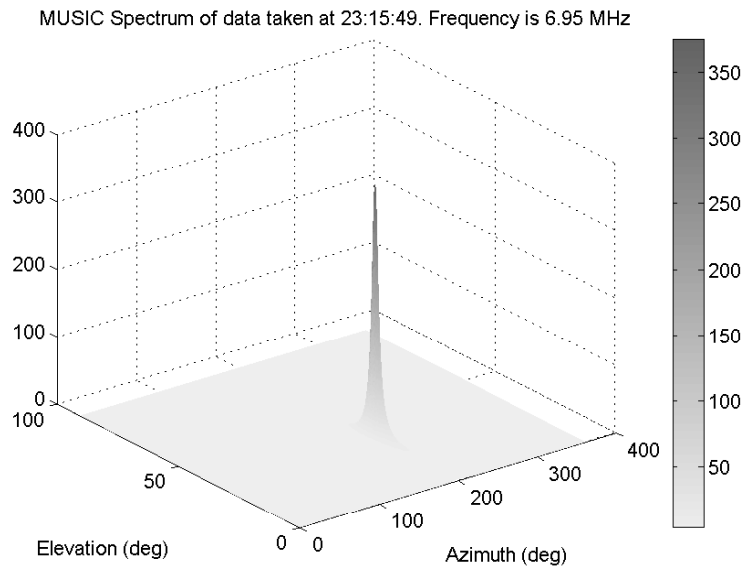


Figure 4.21: MUSIC Spectrum of Data Set 23:15:49.

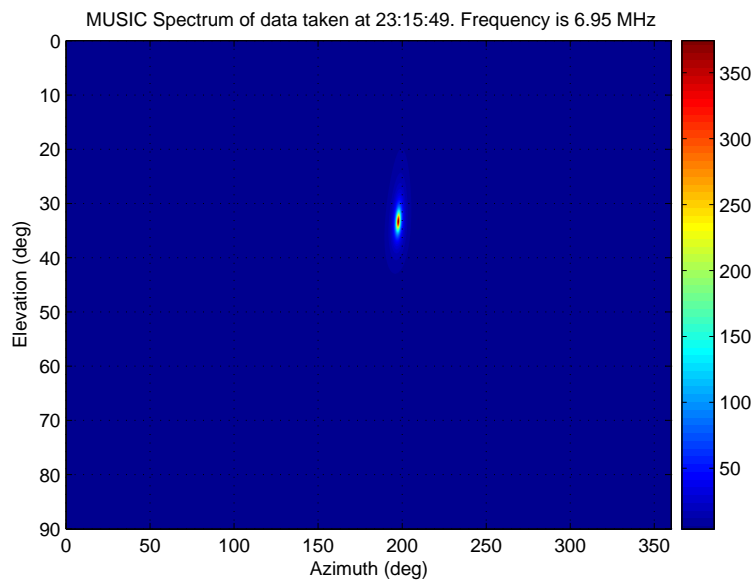


Figure 4.22: MUSIC Spectrum of Data Set 23:15:49.

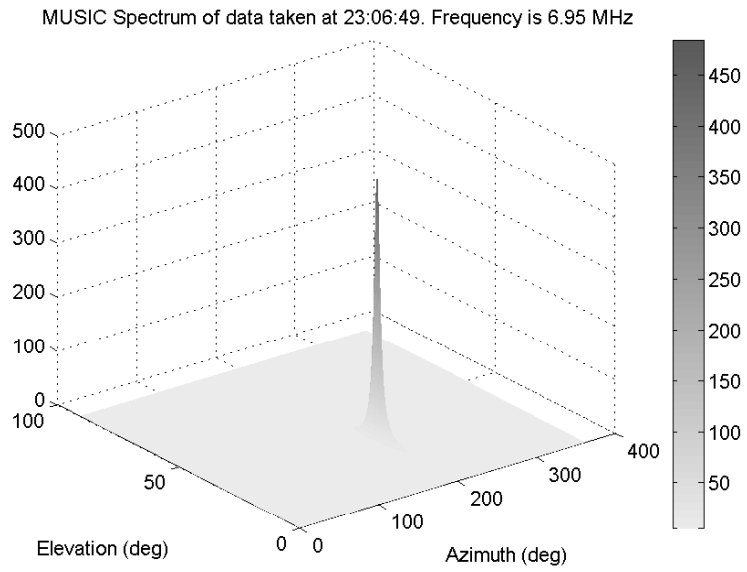


Figure 4.23: MUSIC Spectrum of Data Set 23:06:49.

4.4.4 Data Set 23:06:49

In this section, data set collected at 23:06:49 is used. Open circuit voltage outputs of 5 antenna positioned circularly are used in estimations. Frequency is 6.95MHz . Below figures show the MUSIC method's estimation in 3D and 2D plots. Spectrum clarifies that there is one incoming signal from elevation 31.9° and azimuth 195.7° .

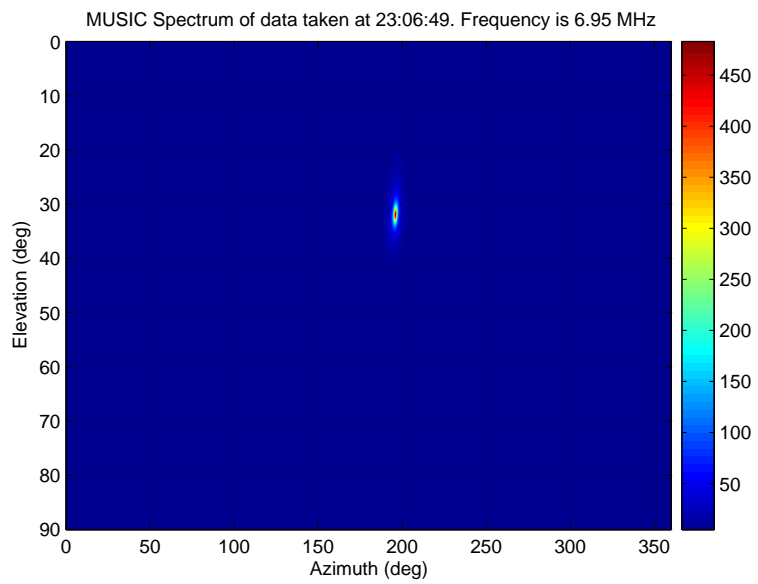


Figure 4.24: MUSIC Spectrum of Data Set 23:06:49.

Chapter 5

Conclusion

Multiple **S**ignal Classification (**MUSIC**) method can be applied to **D**irection **O**f **A**rrival (**DOA**) estimations. Method gives best results when there is only one signals incoming to sensor array that is composed of different numbers of antennas positioned in many different configurations. Different results can be obtained in order to different sensor array configurations such as 2 by 2 planar array configuration, 3 by 3 planar array configuration and V type array configuration. In addition to sensor array configuration, Signal to Noise Ratio is another important parameter in DOA estimations. Method's performance get worse when SNR decreases. Due to the sensor array configuration, minimum SNR level that MUSIC can resolve, can be different. Another parameter for DOA in High Frequency (HF) communication is the condition of ionosphere that is not under control of users. Ionosphere conditions can be defined as good, moderate, poor. Method's performance under the good ionosphere is better than ones under the moderate condition and poor condition.

First of all, algorithm is applied to synthetically obtained open circuit voltages and then applied to open circuit voltages that are obtained by HF waves passed through an ionosphere channel simulator. Effects of ionosphere condition were observed by using the ionosphere simulations.

Method gives better results when the number of antennas is increased. Indeed, increasing number of antennas is not an efficient way for DOA estimation. That's why configurations with different number of antennas are tried in the studies and it is seen that sensor array configuration is more important than number of antennas used in estimations. Average error calculations, standard and mean error calculations shows that V type array configuration with 5 Tripole antennas gives best results when there are incoming signals with very close DOA angles, but when incoming signals are distinct enough V type array configurations with other types of antennas give better results than configurations with Tripole antennas.

Simulations that are made with isotropic antennas when there is one incoming signal, show that MUSIC can resolve clearly at 0 dB SNR level by all array configurations. Within these three array configurations 3 by 3 array configuration gives the best result with 0.175° error. V type 5 array configuration has a worse spectrum than 3 by 3 planar array configuration. V type array configuration has 0.275° error at 0 dB. The worst of three array configurations is 2 by 2 planar array configuration.

Simulations that are made under different ionosphere conditions, different antenna types and different array configurations show that when there are multiple signals incoming to the antenna array, V type configured 5 Tripole antennas give the best result and MUSIC can resolve clearly at 5dB SNR with this setting. If angle difference between signals' arrival angles, gets larger, performance of the configurations gets better. V type array configuration of 5 vertical dipole antennas gives the best result if signals are distinct enough. MUSIC can resolve the spectrum clearly at 0 dB with an error less than 0.5° .

As a future work, comparisons between standard MUSIC algorithm and other spectral or linear algorithms used in DOA estimations can be made. Effects of preprocessing inputs for MUSIC algorithm on the resolution of spectrum and computation time can be observed.

Appendix A

Number of Source Estimation

If the number of sources M is not known, this number must be estimated from data which is the signals induced on the array elements. When the signal power is much larger than the noise power M can be estimated easily from the the eigenvalues of the correlation matrix of data. Eigenvalues show a clear break with the signal eigenvalues larger than noise eigenvalues. In other cases, it may be difficult to determine M just from inspection of eigenvalues[5]. Wax and Kailath developed a formulation of the Akaike Information Criterion (AIC) and the description length (MDL) that is applicable to this situation

$$AIC(M) = -2K(N - M)\ln[Q(M)] + 2M(2N - M)$$

$$MDL(M) = -K(N - M)\ln[Q(M)] + (1/2)M(2N - M)\ln(K)$$

Where $Q(M)$ is the ratio of the geometric mean of the eigenvalues to the arithmetic mean of the eigenvalues

$$Q(M) = \frac{(\lambda_{M+1}\lambda_{M+2}\dots\lambda_N)^{\frac{1}{N-M}}}{\frac{1}{N-M}(\lambda_{M+1} + \lambda_{M+2} + \dots + \lambda_N)}$$

Where K denotes the number of vectors used to find the eigenvalues eg. The number of columns in data matrix Number of M which minimizes the above AIC function is the estimated number of sources.

Appendix B

Standard and Mean Error Calculations For MODLOC 1 and MODLOC 2

B.1 SE and ME Calculations For MODLOC 1

Figures from B.1 to B.9 shows the SE and ME graphics of simulations that are made with MODLOC 1.

B.2 SE and ME Calculations For MODLOC 2

Figures from B.10 to B.18 shows the SE and ME graphics of simulations that are made with MODLOC 2.

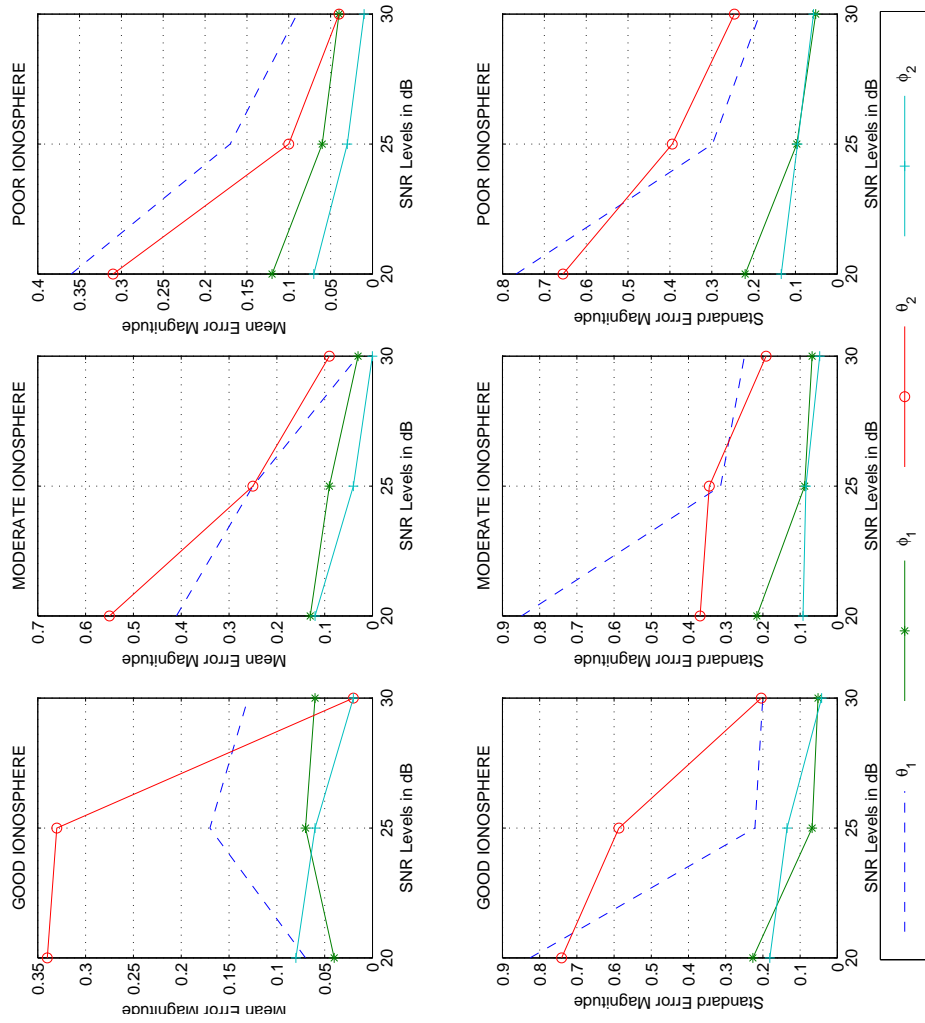


Figure B.1: 2x2 Planar Array with Crossed Loop Antennas for MODLOC 1

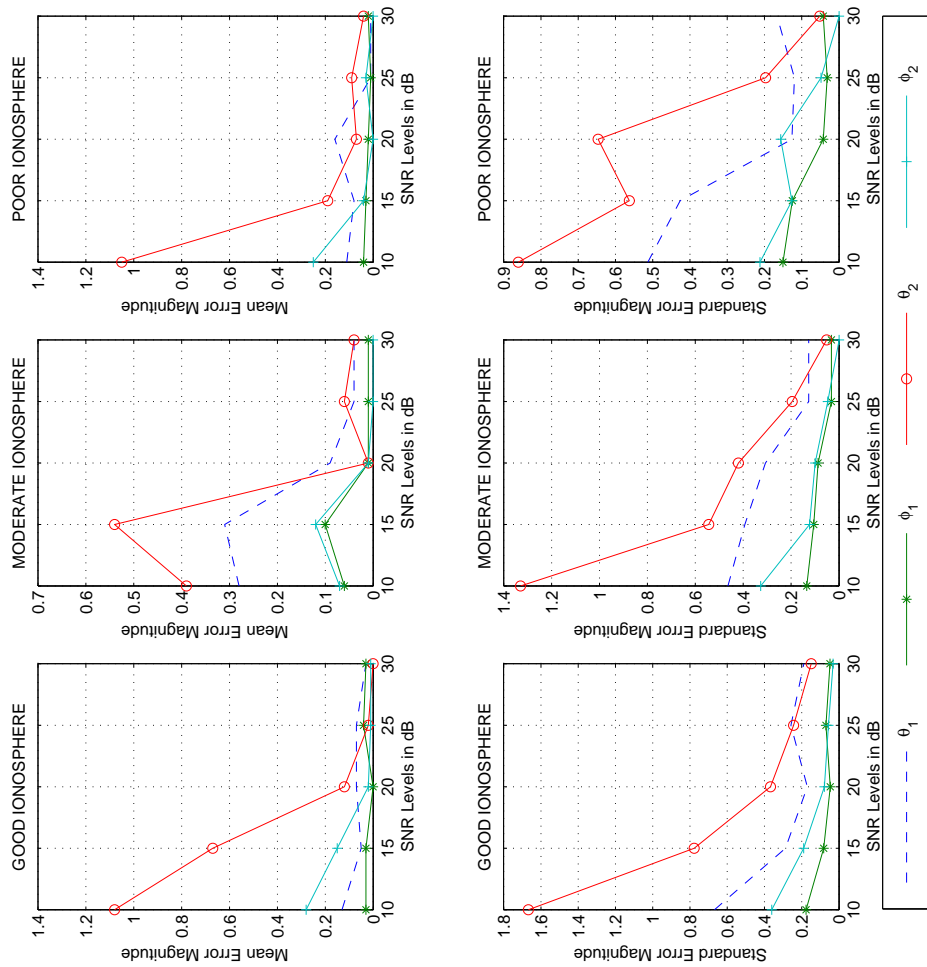


Figure B.2: 2x2 Planar Array with Tripole Antennas for MODLOC 1

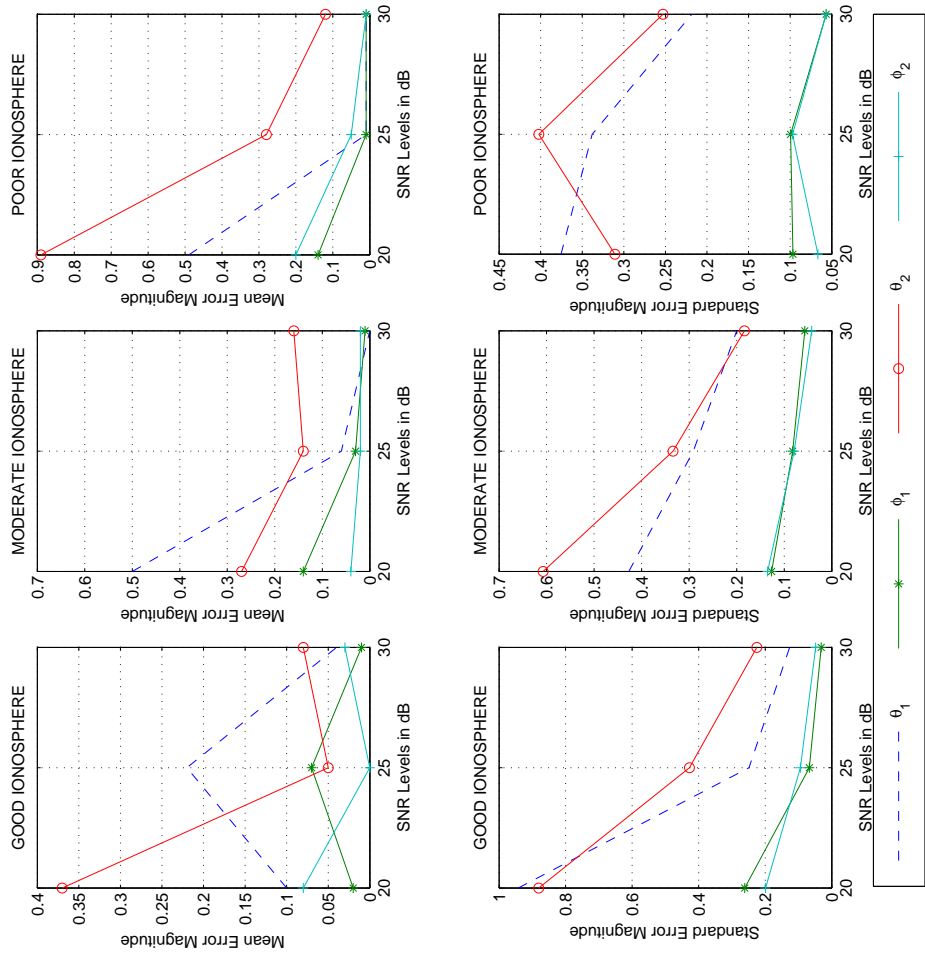


Figure B.3: 2x2 Planar Array with Vertical Dipole Antennas for MODLOC 1

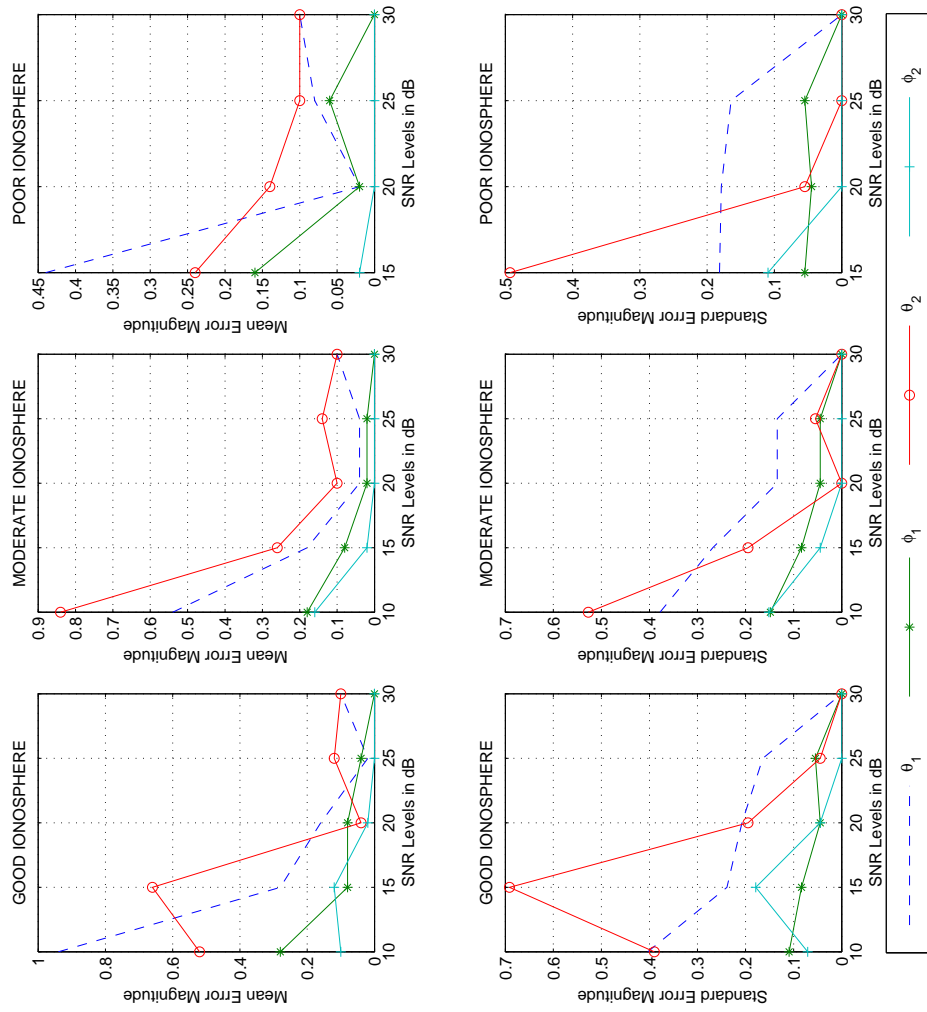


Figure B.4: 3x3 Planar Array with Crossed Loop Antennas for MODLOC 1

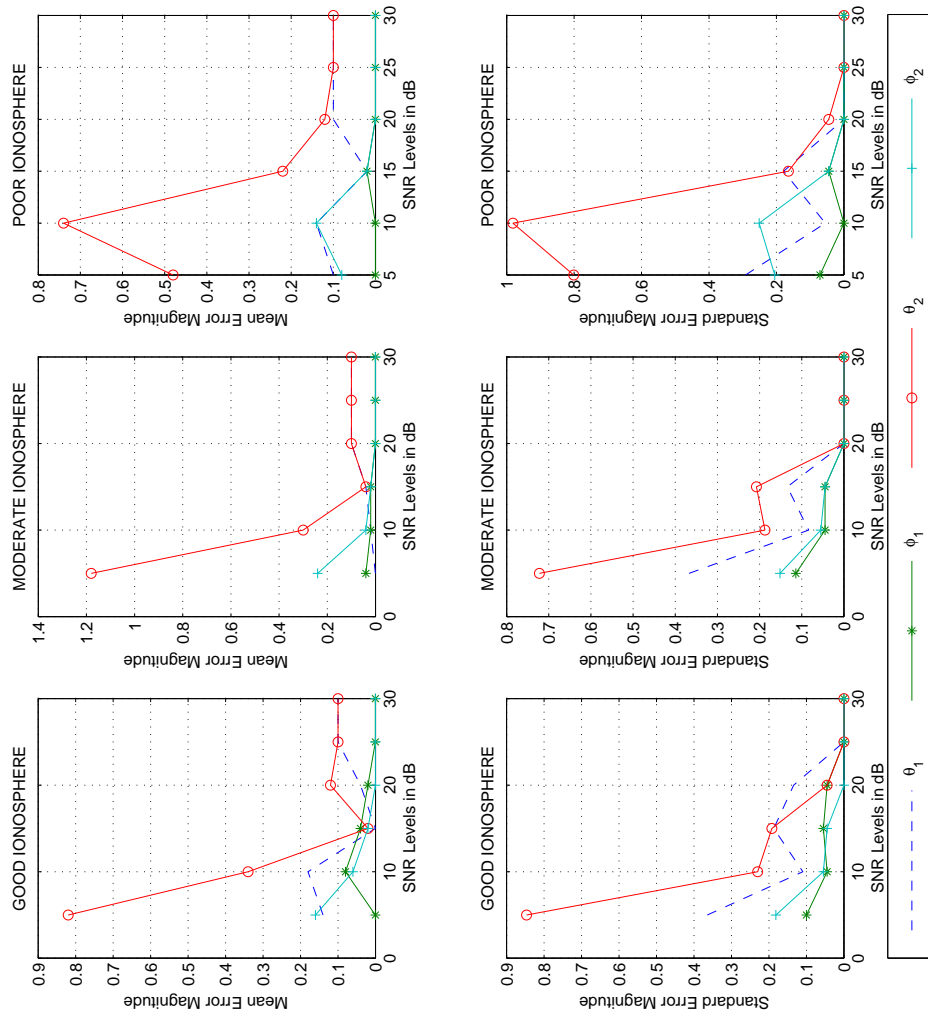


Figure B.5: 3x3 Planar Array with Tripole Antennas for MODLOC 1

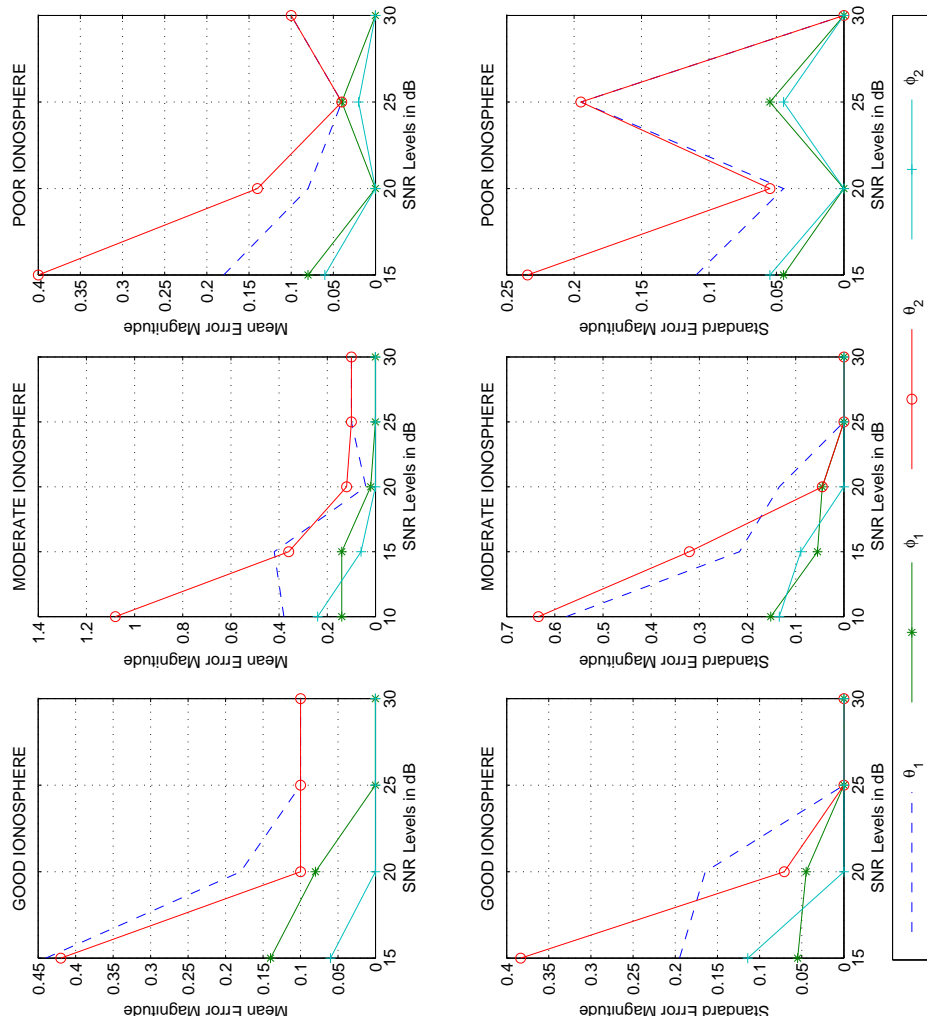


Figure B.6: 3x3 Planar Array with Vertical Dipole Antennas for MODLOC 1

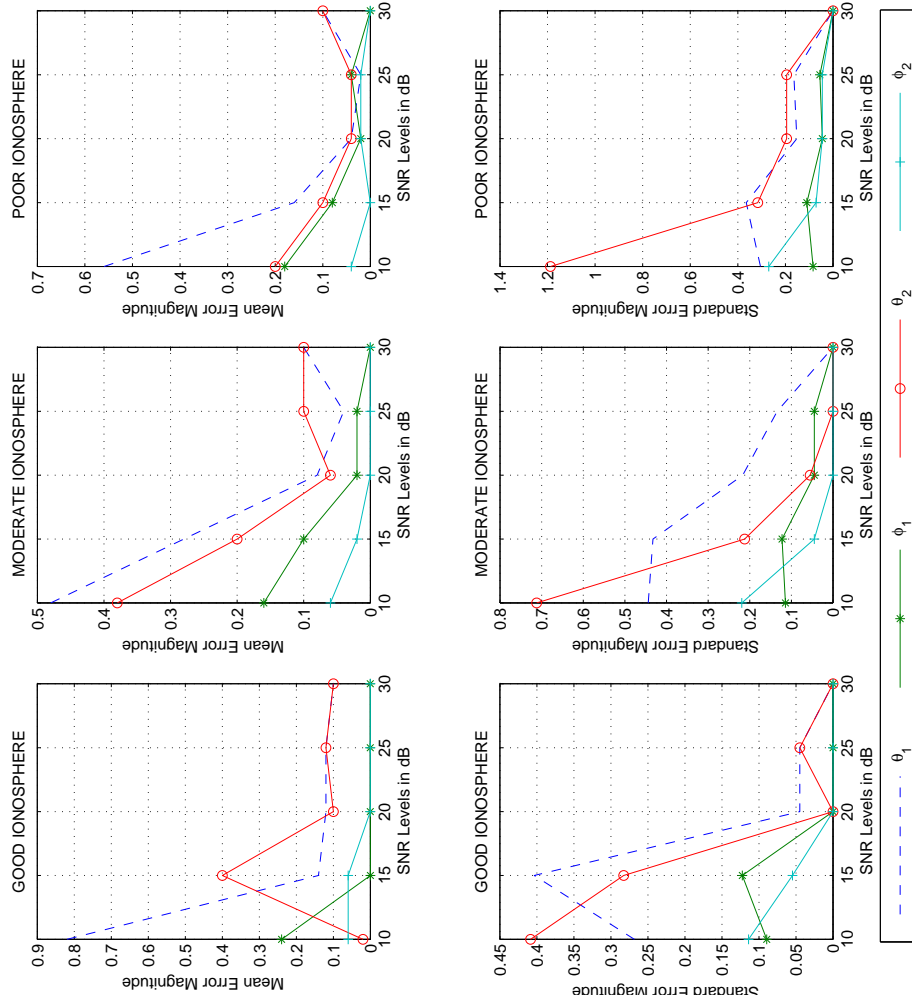


Figure B.7: V type 5 Array with Crossed Loop Antennas for MODLOC 1

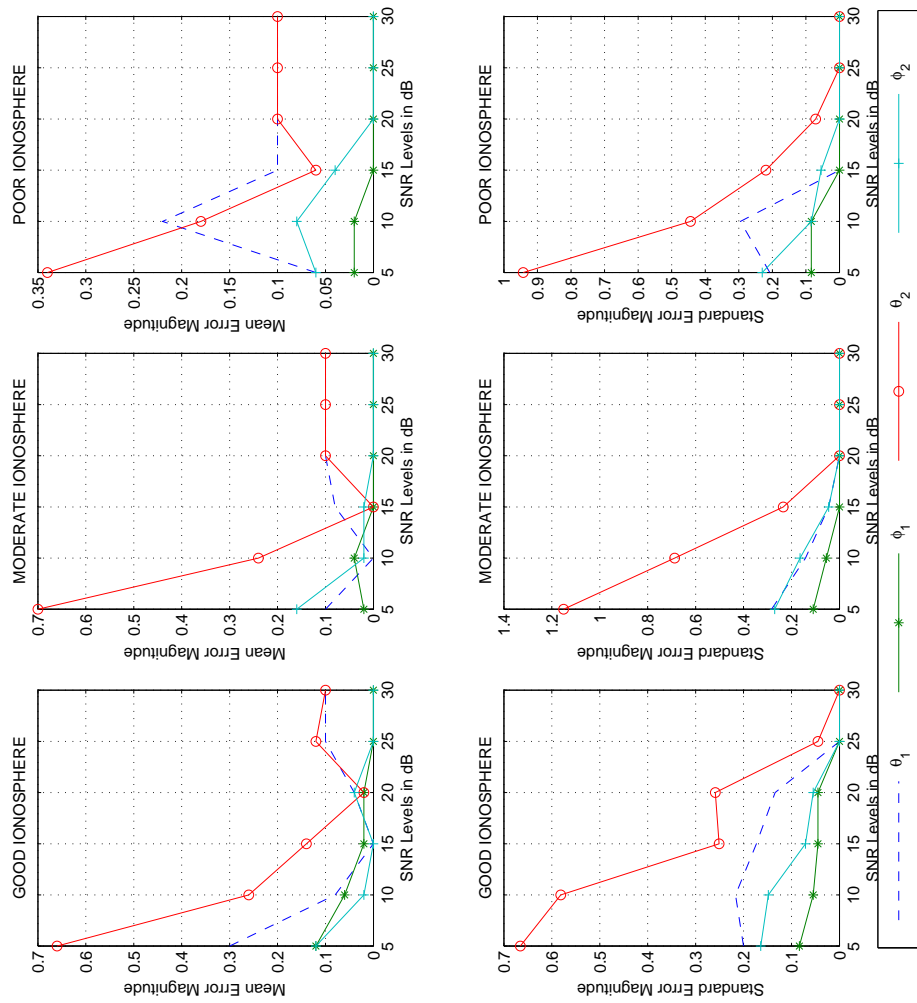


Figure B.8: V type 5 Array with Tripole Antennas for MODLOC 1

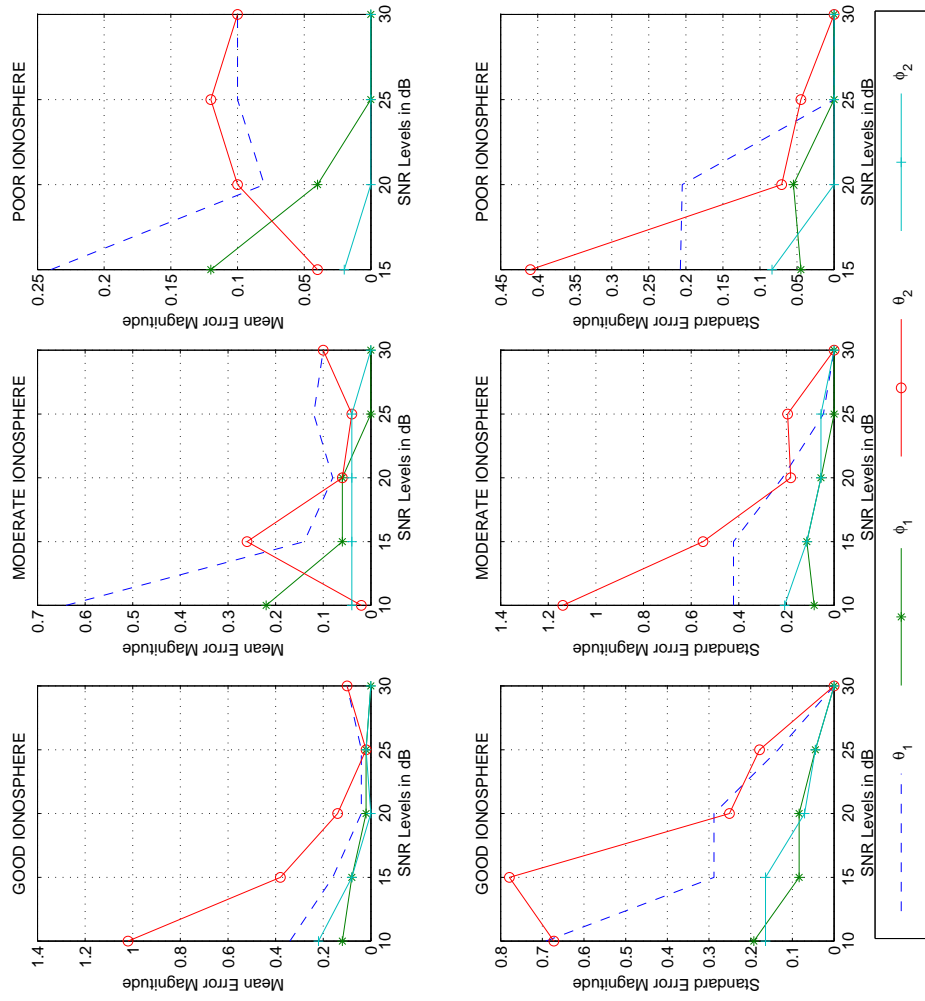


Figure B.9: V type 5 Array with Vertical Dipole Antennas for MODLOC 1

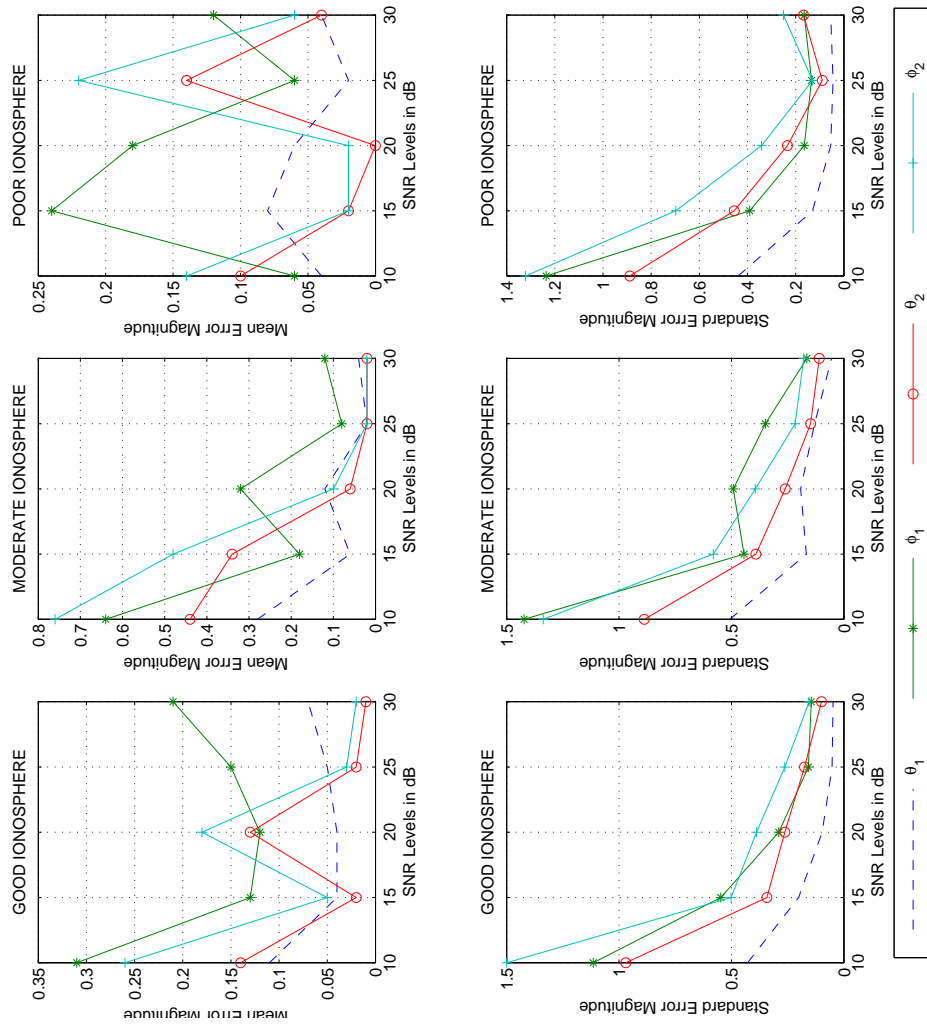


Figure B.10: 2x2 Planar Array with Crossed Loop Antennas for MODLOC 2

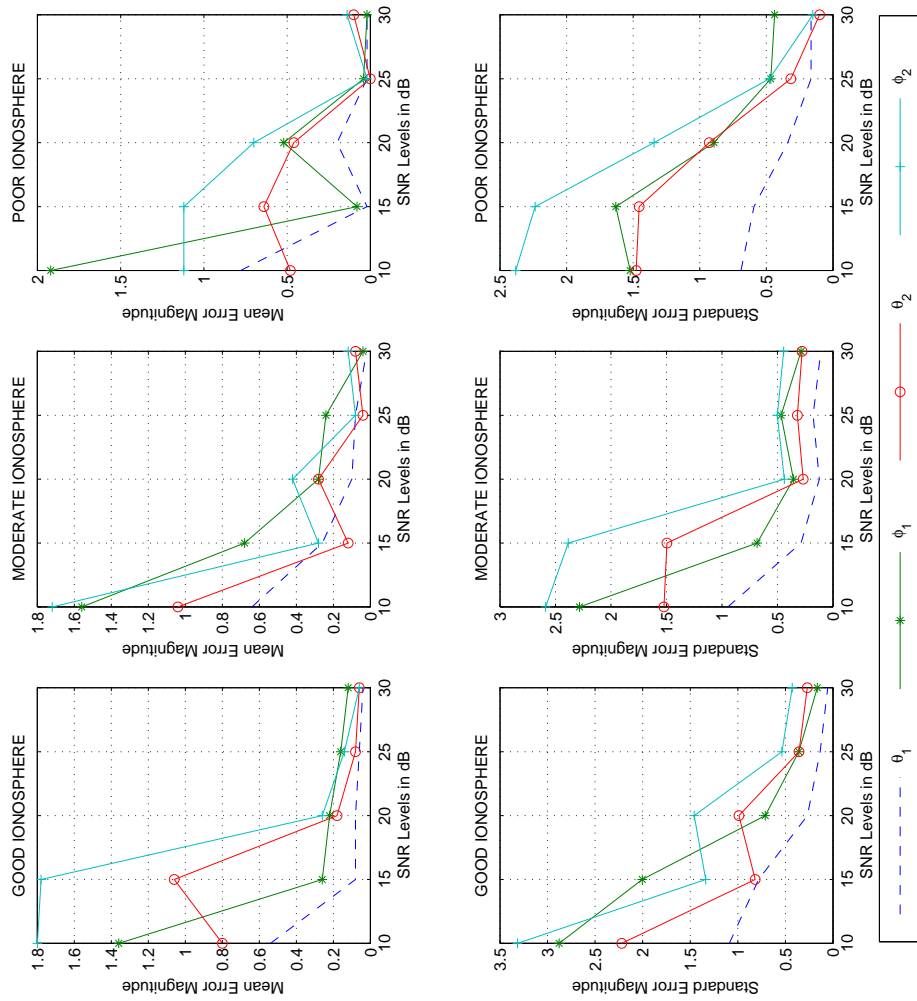


Figure B.11: 2x2 Planar Array with Tripole Antennas for MODLOC 2

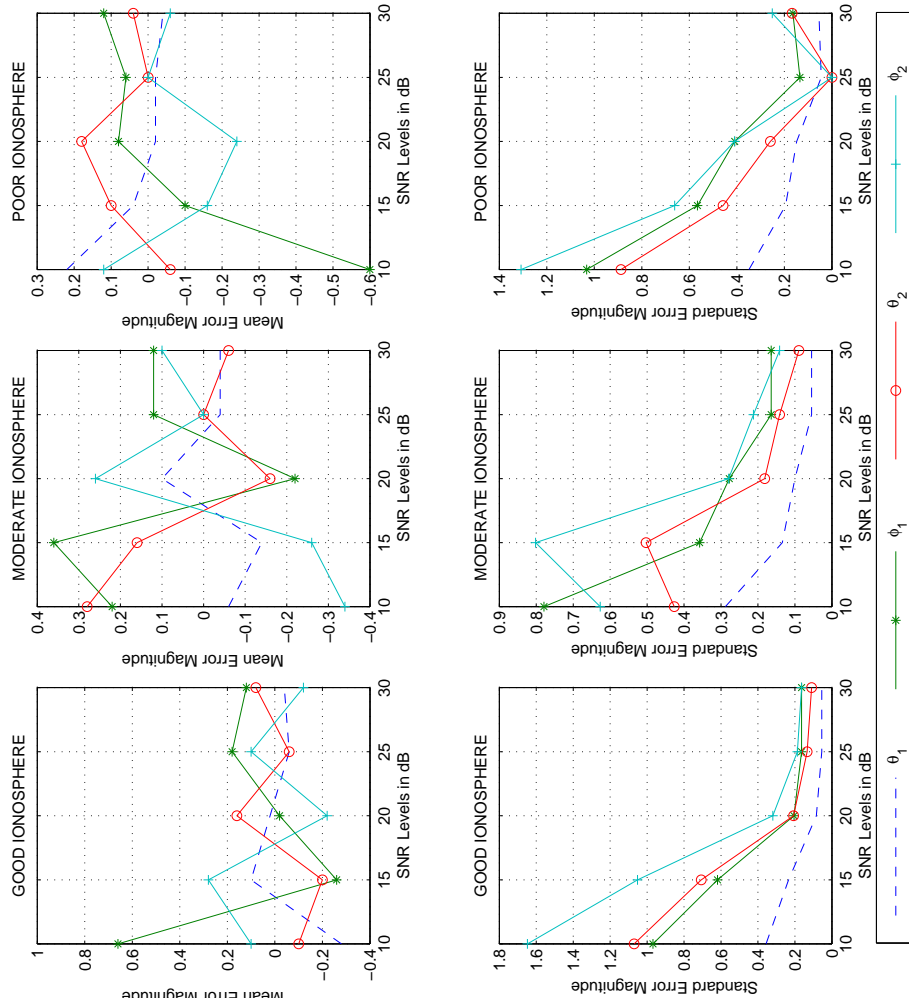


Figure B.12: 2x2 Planar Array with Vertical Dipole Antennas for MODLOC 2

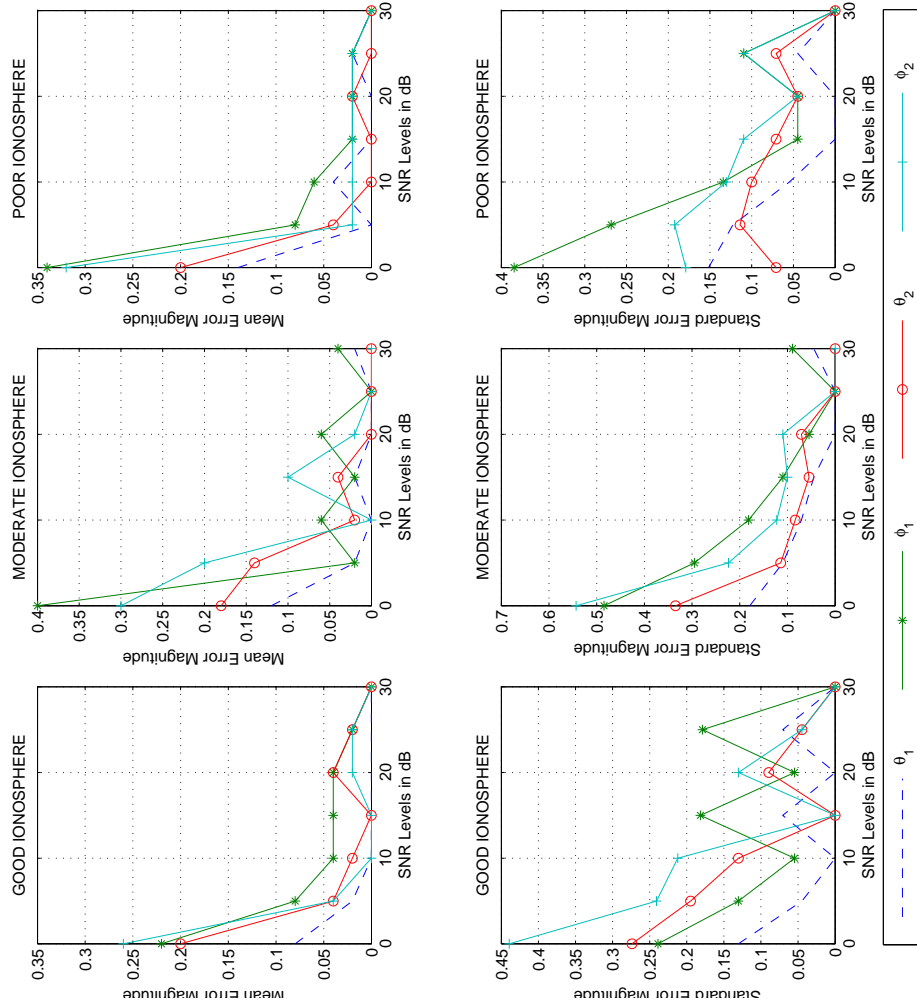


Figure B.13: 3x3 Planar Array with Crossed Loop Antennas for MODLOC 2

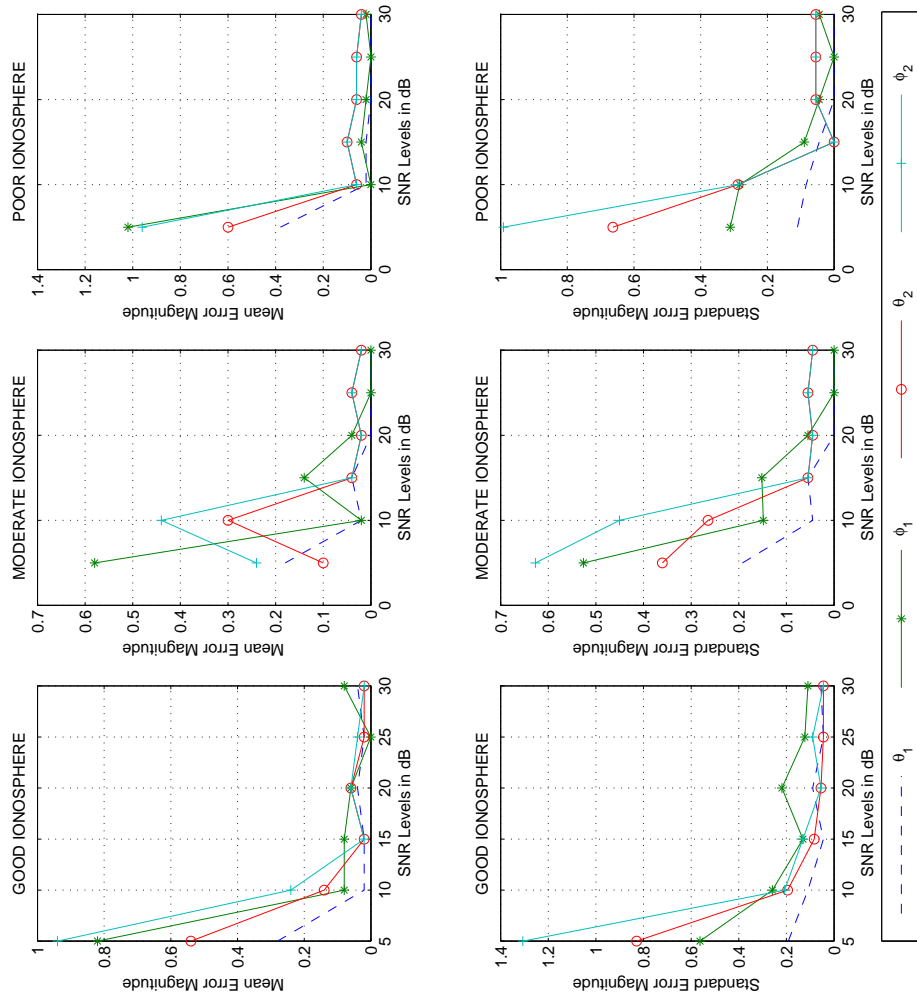


Figure B.14: 3x3 Planar Array with Tripole Antennas for MODLOC 2

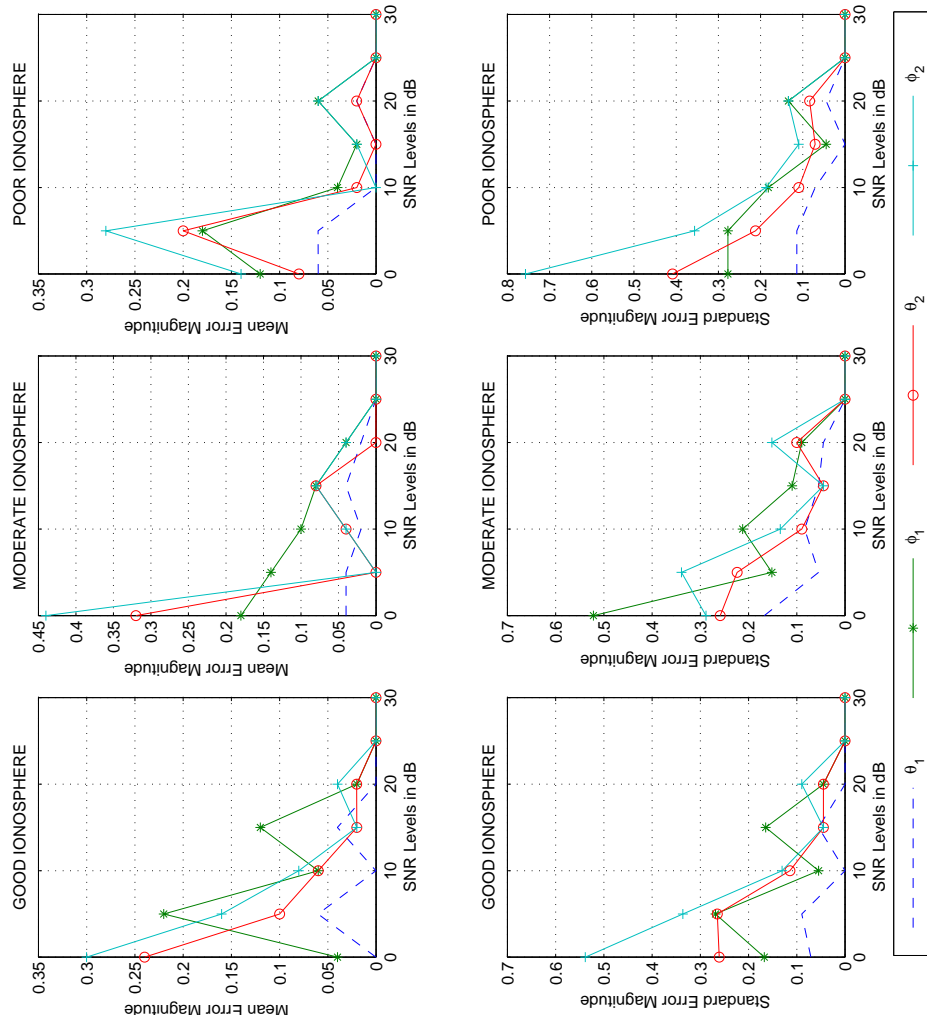


Figure B.15: 3x3 Planar Array with Vertical Dipole Antennas for MODLOC 2

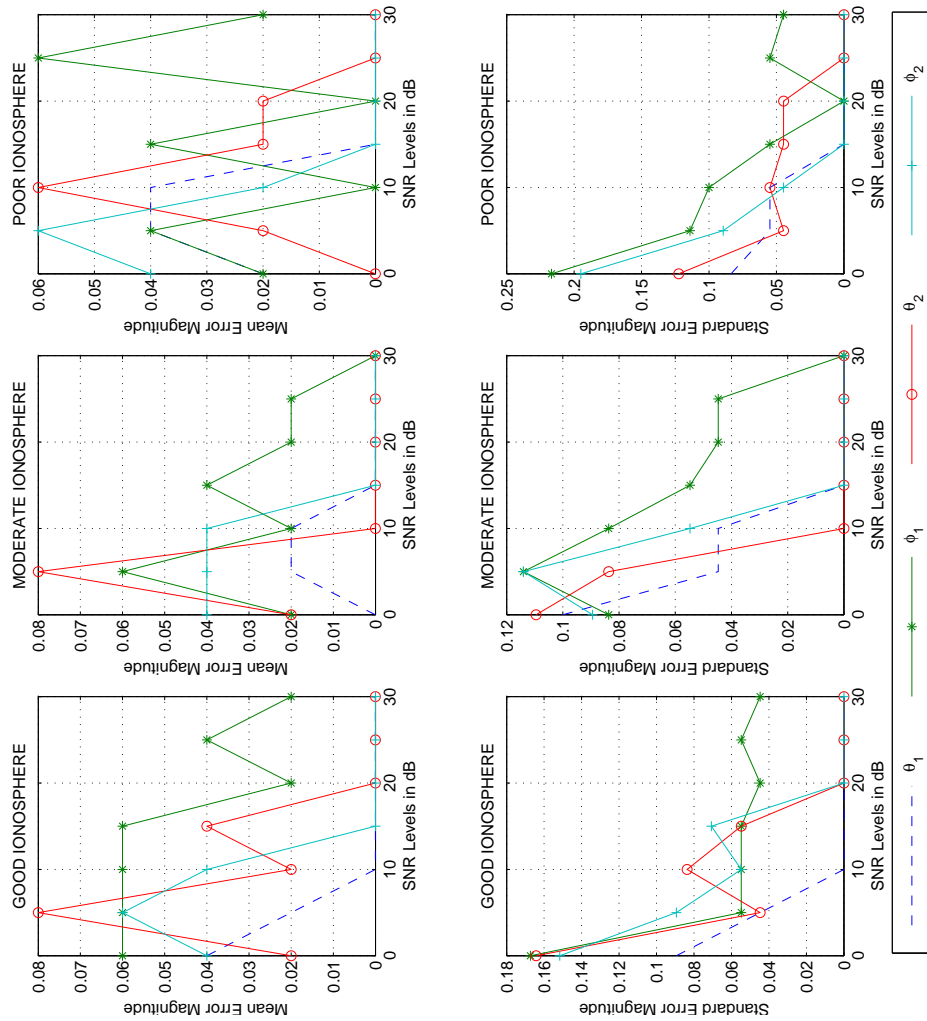


Figure B.16: V type 5 Array with Crossed Loop Antennas for MODLOC 2

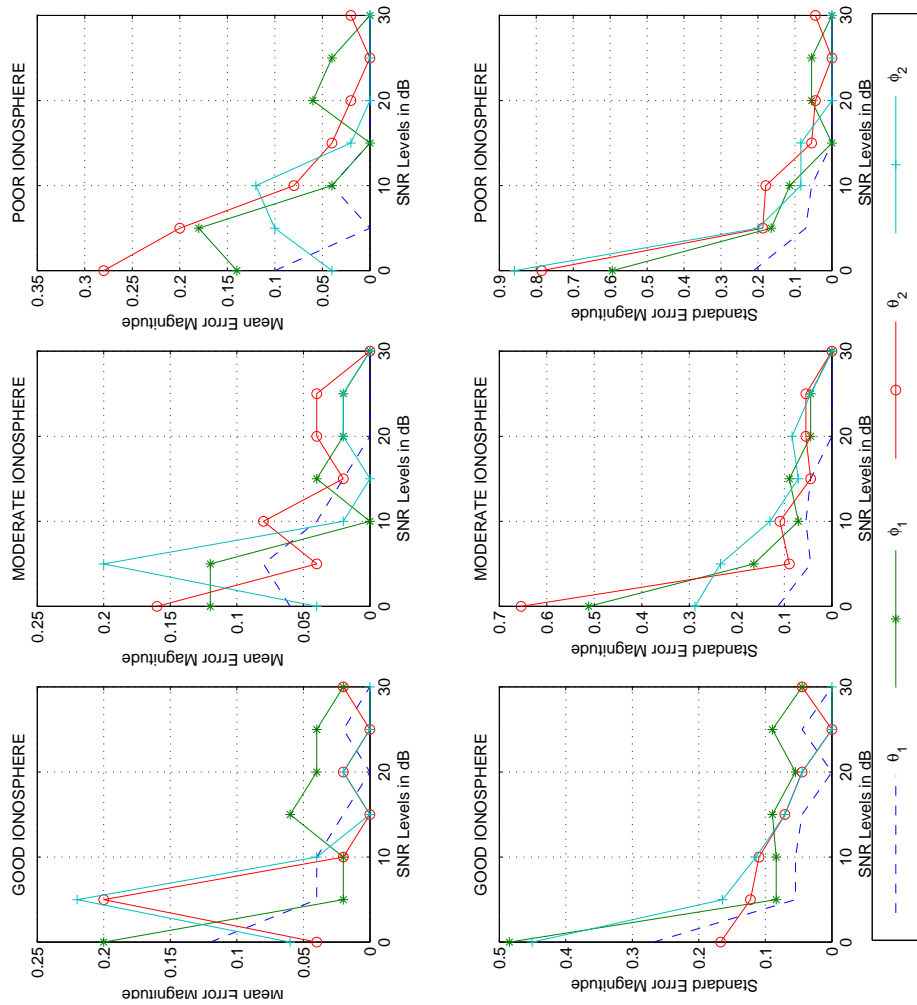


Figure B.17: V type 5 Array with Tripole Antennas for MODLOC 2

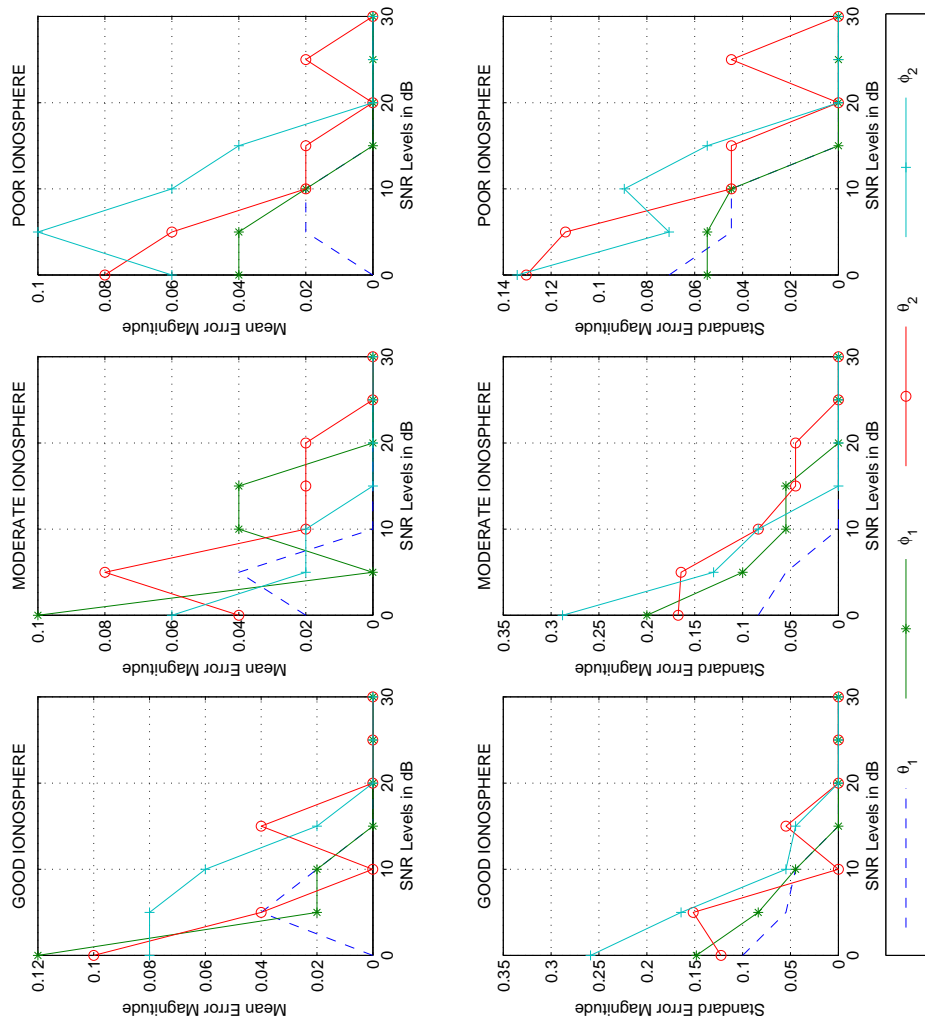


Figure B.18: V type 5 Array with Vertical Dipole Antennas for MODLOC 2

Bibliography

- [1] Olfat A.,Esfahani Said N.,High Resolution Direction Of Arrival Estimation,Department of Electrical Engineering Tehran University, Tehran 14395, Iran.
- [2] Godara, Lal Chand, "Smart Antennas", Boca Raton, Fla, CRC Press,2004.
- [3] Godara, Lal Chand, Application of antenna arrays to mobile communications, part II: Beam forming and direction of arrival considerations, Proc. IEEE, 85, 1193-1245, 1997.
- [4] Adve R., 2003, Direction Arrival Estimation., Toronto.
- [5] Taskin A., 1999, Performance comparison of two direction of arrival angle estimation methods: Delay and Sum Beamforming, Multiple Signal Classification (MUSIC).